

5-2010

Regenerating Spent Zeolites with UV and UV/ H₂O₂ To Enhance Removal of Endocrine Disrupting Compounds

Safina Singh

Follow this and additional works at: https://scholarworks.umass.edu/cee_ewre

 Part of the [Environmental Engineering Commons](#)

Singh, Safina, "Regenerating Spent Zeolites with UV and UV/H₂O₂ To Enhance Removal of Endocrine Disrupting Compounds" (2010). *Environmental & Water Resources Engineering Masters Projects*. 38.
<https://doi.org/10.7275/G96G-2773>

This Article is brought to you for free and open access by the Civil and Environmental Engineering at ScholarWorks@UMass Amherst. It has been accepted for inclusion in Environmental & Water Resources Engineering Masters Projects by an authorized administrator of ScholarWorks@UMass Amherst. For more information, please contact scholarworks@library.umass.edu.

**REGENERATING SPENT ZEOLITES WITH UV AND UV/H₂O₂ TO ENHANCE
REMOVAL OF ENDOCRINE DISRUPTING COMPOUNDS**

A Project Presented

By

Safina Singh

Master of Science in Environmental Engineering

Department of Civil and Environmental Engineering
University of Massachusetts
Amherst, MA 01003

May 14, 2010

**REGENERATING SPENT ZEOLITES WITH UV AND UV/H₂O₂ TO ENHANCE
REMOVAL OF ENDOCRINE DISRUPTING COMPOUNDS**

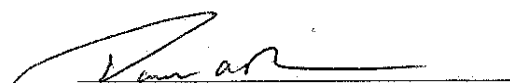
A Masters Project Presented

by

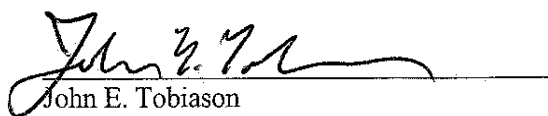
Safina Singh

Approved as to style and content by:


Erik J. Rosenfeldt, Chairperson


David A. Reckhow, Member


Robert W. Thompson, Member


John E. Tobiason
Graduate Program Director, MSEVE
Civil and Environmental Engineering Department

ACKNOWLEDGEMENTS

I would like to thank my advisor Dr. Erik J. Rosenfeldt for his time, knowledge, encouragement and support during my study. Many thanks to Dr. John E. Tobiason for his guidance and support during the course of my masters here at the University of Massachusetts. I would like to thank Dr. Sarina J. Ergas for her support during my stay at UMass-Amherst as a dual-degree student. I would also like to extend my appreciation to Dr. David Reckhow and Dr. Robert Thompson for sitting on my committee and other professors at UMass who have shared their knowledge and expertise through the classes they taught me.

Last but not the least; I would like to express my gratitude to my colleagues in the department and my friends in the area who have made living in Amherst enjoyable. Also, I want to take this opportunity to thank my family who has always supported and encouraged me to move forward.

ABSTRACT

Endocrine disrupting compounds (EDCs) have become contaminants of emerging concern due to their potential for harmful effects on human and ecological health, at low concentrations (ppb). As an alternative to conventional adsorption media, activated carbon, this study investigates feasibility of using high-silica, hydrophobic zeolites for the removal of EDCs through adsorption process. Zeolites are crystalline, porous alumino-silicate with well defined pore structures, and tetrahedral framework.

While traditional media regeneration processes are energy and cost intensive, evidence has been found that zeolites can be regenerated multiple times through relatively inexpensive methods using direct ultraviolet (UV) photolysis and advanced oxidation process (AOP). The regeneration process not only presents potential for multiple uses of the sorption media, but provides the additional benefit of oxidative treatment of back wash water produced from zeolite regeneration, potentially generating less hazardous waste.

Bench scale adsorption studies were performed to collect baseline adsorption data for three EDCs; estrone (E1), 17- β Estradiol (E2) and 17- α Ethinylestradiol, on three zeolites; CBV-400, CBV-780 and CBV-901. Freundlich and Langmuir isotherms models were considered to estimate the adsorption capacity and strength of each of these zeolites for the selected EDCs.

CBV-400 showed minimal adsorption of all three EDCs and hence was disregarded for kinetic and regeneration experiments. For CBV-780 and CBV-901, results obtained

showed that equilibrium was reached within an hour, and over 90% of the EDCs were typically removed within 10 minutes of the reaction time.

Polychromatic, Medium Pressure Ultraviolet (MP UV) energy was used for the regeneration experiment due to the relatively high quantum yield of the EDCs being studied as compared to monochromatic, Low Pressure UV (LP UV). Results showed that regenerating zeolites with UV and UV/H₂O₂ treatment can more than double their adsorption capacity after four regeneration cycles when compared to untreated zeolites. Regeneration using advanced oxidation process with peroxide (UV/H₂O₂) did not significantly improve regeneration efficiency of zeolites compared to UV photolysis.

Studies were also conducted to evaluate the adsorption capacity of the zeolites in natural water. Lower adsorption of EDCs was achieved in natural water than in deionized water which was attributed to interference of various anions, cations and other precipitate salts depositing on the surface of zeolites.

TABLE OF CONTENTS

ACKNOWLEDGEMENTS	iii
ABSTRACT	iv
TABLE OF CONTENTS	vi
LIST OF TABLES	ix
LIST OF FIGURES	x
1. LITERATURE REVIEW	1
1.1. Endocrine Disrupting Compounds	1
1.1.1. Effects of EDCs	1
1.1.2. Sources of EDCs	3
1.1.3. EDCs Studied	4
1.2. Ultraviolet (UV) Based Processes for Transforming EDCs	5
1.2.1. Ultraviolet (UV) Radiation in Water Treatment (Disinfection)	5
1.2.2. UV Photolysis for Chemical Treatment	10
1.2.3. UV Based Advanced Oxidation Process	12
1.2.4. Removal of EDC activity with UV AOP	14
1.3. Zeolite Media Adsorption	15
1.3.1. Characteristics of Zeolites	16
1.3.2. Zeolites for Removal of Organic Contaminants in Water	19
1.3.3. Potential for Zeolite Regeneration	21
2. INTRODUCTION	23
2.1. Problem Statement	23

2.2. Objectives.....	24
3. MATERIAL AND METHODS OF INVESTIGATION.....	25
3.1. Chemicals, Materials and Equipments.....	25
3.2. Experimental Design.....	27
3.2.1. Water Samples.....	27
3.2.2. Adsorbent.....	28
3.2.3. Adsorption Equilibrium.....	28
3.2.4. Adsorption Kinetics.....	30
3.2.5. Zeolite Media Regeneration.....	31
3.2.6. UV Irradiation Procedure.....	33
3.3. Adsorption and Regeneration in Estrogen Spiked Natural Waters.....	34
3.4. Analytical Methods.....	35
4. RESULTS AND DISCUSSIONS.....	37
4.1. Kinetics of Adsorption.....	38
4.2. Adsorption Equilibrium.....	40
4.2.1. The Langmuir Isotherm.....	41
4.2.2. The Freundlich Isotherm.....	42
4.2.3. Adsorption of the estrogens on the zeolite CBV-780.....	45
4.2.4. Adsorption of the estrogens on the zeolite CBV-901.....	51
4.2.5. CBV-780 versus CBV-901.....	55
4.3. Regenerative Ability of Zeolites.....	58
4.4. Dose Response in Regeneration.....	64
4.5. Adsorption in Natural Waters.....	69
5. SUMMARY AND CONCLUSIONS.....	77

6. FUTURE INVESTIGATIONS	79
7. REFERENCES	80
Appendix A – Suppliers Information on the Zeolites Tested	87
APPENDIX B – Medium Pressure Lamp.....	90
APPENDIX C – MP UV Photolysis of EDCs selected	91
APPENDIX D – E1, E2 and EE2 Calibration Curves	93
APPENDIX E – Detection Limit of Water Quality Analysis Equipments Used	95

LIST OF TABLES

Table 1.1 Properties of E2, EE2 and E1 (Hanselman <i>et al.</i> , 2003; Lai <i>et al.</i> , 2000)	4
Table 1.2 Typical mercury vapor lamp characteristics (USEPA, 2006).....	7
Table 1.3 Disinfection UV Dose requirements in millijoules per centimeter squared (mJ/cm ²) ¹	10
Table 1.4 Properties of zeolites used as adsorbent.	18
Table 3.1 List of chemicals used in the study	25
Table 3.2 List of materials and equipments	26
Table 3.3 Typical zeolites concentration used for adsorption equilibrium experiments ..	29
Table 4.1 Summary of adsorption isotherm parameters for CBV-780	47
Table 4.2 Summary of adsorption isotherm parameters for CBV -901	55
Table 4.3 UV irradiation times and the corresponding UV dose.....	66
Table 4.4 Water quality parameters (all in mg/L) of natural water samples	70
Table 4.5 Water quality analysis of post-filter and raw water before and after adsorption equilibrium experiments with zeolite CBV-780	72
Table 4.6 Freundlich and Langmuir parameters for deionized and natural waters	75

LIST OF FIGURES

Figure 1.1 Molecular structures of E1, E2 and EE2	4
Figure 1.2 Relative Emission Spectra from Low (LP-UV) and Medium Pressure (MP-UV) UV Lamps as Compared to the Absorbance Spectrum of DNA (Sharpless, 2001).....	8
Figure 1.3 Absorption of E1 (from this study), E2, EE2, and H ₂ O ₂ over the UV spectrum (UVC = 200-280nm, UVB = 280-315nm). The molar absorption coefficients of H ₂ O ₂ have been multiplied by 10 to display them on the same graph (Based on Rosenfeldt and Linden, 2004).....	11
Figure 1.4 Natural zeolites: a) Chabazite; b) Clinoptilolite; c) Faujasite; d) tetrahedral framework found on Faujasite	17
Figure 1.5 Primary building blocks of zeolites (Bhatia, 1990).....	18
Figure 1.6 Sodalite cage structure (Bhatia, 1990).....	18
Figure 3.1 Regeneration of zeolites	31
Figure 4.1 Adsorption of EE2 on all three zeolites, CBV-400, -780 and -901.....	37
Figure 4.2 Kinetics of reaction for the adsorption of E1 on CBV-780 and -901.....	39
Figure 4.3 Kinetics of reaction for the adsorption of E2 on CBV-780 and -901.....	39
Figure 4.4 Kinetics of reaction for the adsorption of EE2 on CBV-780 and -901	40
Figure 4.5 Typical isotherms describing sorption of organic compounds in water and vapor phase (BET) by natural sorbents (Delle Site, 2001).	44
Figure 4.6 Adsorption isotherms of E1, E2 and EE2 on CBV-780	45
Figure 4.7 The linearized Freundlich isotherms of E1, E2 and EE2 on CBV-780.....	46
Figure 4.8 The linearized Langmuir isotherms of E1, E2 and EE2 on CBV-780	46
Figure 4.9 Adsorption isotherms of E1, E2 and EE2 on CBV-901	51
Figure 4.10 Comparison of adsorption equilibrium data from Wen <i>et al.</i> (2009) with values obtained in this study	52
Figure 4.11 The linearized Freundlich isotherms of E1, E2 and EE2 on CBV-901.....	53
Figure 4.12 The linearized Langmuir isotherms of E1, E2 and EE2 on CBV-901	54
Figure 4.13 Remaining E1 concentration during UV photolysis and UV AOP as compared to untreated zeolites case	59

Figure 4.14 Comparison of cumulative E1 mass adsorbed by zeolites treated with UV and UV AOP; and untreated zeolites	60
Figure 4.15 Remaining E2 concentration during UV photolysis and UV AOP as compared to untreated zeolites case	61
Figure 4.16 Comparison of cumulative E2 mass adsorbed by zeolites treated with UV and UV AOP; and untreated zeolites	62
Figure 4.17 Remaining EE2 concentration during UV photolysis and UV AOP as compared to untreated zeolites case	63
Figure 4.18 Comparison of cumulative EE2 mass adsorbed by zeolites treated with UV and UV AOP; and untreated zeolites	64
Figure 4.19 Comparison of E2 degradation between different UV irradiation times.....	66
Figure 4.20 Comparison of cumulative E2 mass adsorbed by zeolites treated with 30 to 5 minutes of UV	67
Figure 4.21 Remaining E2 concentration in UV/H ₂ O ₂ and UV treatment compared to control experiment.....	68
Figure 4.22 Comparison of cumulative E2 mass adsorbed by zeolites treated with UV and UV AOP; and untreated zeolites	69
Figure 4.23 Adsorption isotherms of E2 on CBV-780 in DI and natural waters.....	70
Figure 4.24 The linearized Freundlich isotherm of adsorption of E2 in natural water on CBV-780	73
Figure 4.25 The linearized Langmuir isotherm of adsorption of E2 in natural water on CBV-780	74

1. LITERATURE REVIEW

1.1. Endocrine Disrupting Compounds

As the name implies endocrine disrupting compounds (EDCs) adversely affect the physiologic endocrine system consisting of the thyroid system, metabolism, and reproductive system. These compounds have been known to interfere with hormonal signals whose chronology and dose can permanently affect future form and functions of many tissues (Colborn *et al.*, 1993; Health Canada, 1999; Auriol *et al.*, 2006). A wide range of compounds, both natural and synthetic, have been classified as EDCs. Three main categories of EDCs include, estrogenic, androgenic and thyroid. Estrogenic compounds mimic or block natural estrogen. Likewise, androgenic compounds mimic or block natural testosterone. Thyroid compounds directly or indirectly impact thyroid system (Snyder *et al.* 2003).

1.1.1. Effects of EDCs

EDCs can affect endocrine system and organs during prenatal and postnatal life. Offspring can be directly exposed to these compounds after birth or indirectly via exposure of the mother at any time throughout her life, as EDCs can accumulate in body fat which is utilized during egg laying or pregnancy and lactation (Colborn *et al.*, 1993). Effect of exposure to EDCs can be expressed at any developmental stage of an organism. It may have permanent consequences in the early embryo or fetus, or can affect the course of development. EDCs may act through multiple mechanisms and may only be expressed during certain developmental periods. Some responses of

EDCs may be delayed and may not surface fully until later stages of life (Colborn *et al.* 1993).

Over the past decade, a growing number of studies have suggested adverse effects of EDCs in many wildlife species of fish, reptiles, birds and mammals (Van den Belt *et al.*, 2004). Exposure to endocrine-disrupting chemicals in the environment has been associated with abnormal thyroid function and decreased fertility in birds, fish, shellfish and mammals. EDCs have been also known to cause demasculinization and feminization of male fish, birds and mammals; defeminization and masculinization of female fish and birds; and alteration of immune function in mammals (Colborn *et al.*, 1993).

In wildlife species, maternal transfer of EDCs with subsequent effects in offspring has been proven experimentally. In humans, a study showed that daughters of the mothers who were exposed to Diethylstilbestrol (DES), a synthetic estrogen, revealed reproductive organ dysfunction, abnormal pregnancies, a reduction in fertility, immune system disorders and periods of depression (Colborn *et al.*, 1993; Takasugi and Bern, 1988). EDCs are lipid soluble and many of them have been reported in organs of the body and fatty tissues including the reproductive tissues of men and women. Breast milk has high lipid content, thus a major concern has been bioaccumulation of EDCs in breast milk. It has been documented that the infant is exposed to high concentrations of many of these chemicals during breastfeeding (Johnson-Restrepo *et al.*, 2007; Colborn *et al.*, 1993). Environmental exposure of EDCs has also been associated with increased cases of pathologies after the early 1970's in men and women, including prostatic and breast cancer, benign prostatic

hyperplasia, cancers of estrogen-responsive tissues in women (vaginal, cervical and endometrial), ectopic pregnancies, cryptorchidism (Colborn *et al.*, 1993).

1.1.2. Sources of EDCs

Natural sources of EDCs include urine and feces from mammals including humans. Although these natural EDCs have always been in the environment, growing global population and livestock-farming practices have caused the levels of these compounds to increase steadily over the years (López de Alda and Barceló, 2001). A wide variety of manufactured chemicals constitute endocrine disrupting compounds. Some of the sources of EDCs include herbicides (e.g. Atrazine), fungicides (e.g., Benomyl), insecticides (e.g. DDT, Dicofol); and industrial chemicals such as cadmium, dioxin, PCBs, Phthalates. Some PCBs are directly estrogenic while others become estrogenic after *in vivo* conversion (Colborn *et al.*, 1993). PCBs and DDT are persistent compounds and can remain in the environment over geologic time. During transport of these chemicals over a long distance, a significant amount can be released into the atmosphere which can be sequestered into water bodies. The Great Lakes in North America accumulated a considerable amount of such EDCs via sequestration from atmosphere. EDCs are neither mutagens nor acute toxicants at ambient concentrations and hence can be released without proper caution into the environment (Colborn *et al.*, 1993).

1.1.3. EDCs Studied

Three EDCs- estrone (E1), 17- β -estradiol (E2) and 17- α -ethinyl estradiol (EE2) illustrated in Figure 1.1, were selected for the study. E1 and E2 are natural hormones whereas; EE2 is synthetic and is an active ingredient in many oral contraceptives for women. These compounds are commonly called estrogens as they are steroidal compounds that function as the primary female sex hormones. Estrogens are characterized by low volatility, low solubility and high affinity for organic matter, as described by the properties shown in Table 1.1.

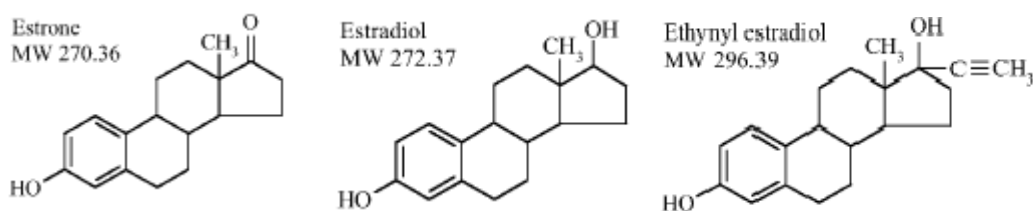


Figure 1.1 Molecular structures of E1, E2 and EE2

(Source: López de Alda and Barceló, 2001)

Table 1.1 Properties of E2, EE2 and E1 (Hanselman *et al.*, 2003; Lai *et al.*, 2000)

Compound	Solubility (mg/L) in DI @ T (°C)	pK _a	Log K _{ow}	Melting Pt. (°C) ¹	Molecular Wt. (g/mol)
Estrone (E1) C ₁₈ H ₂₂ O ₂	30 @ 25°C ¹ 13 @ 20°C	10.3-10.8	3.13 (3.13 – 3.4)	255	270.4
17- β -estradiol (E2) C ₁₈ H ₂₄ O ₂	3.6 @ 27°C ¹	10.5-10.7	4.01 (3.57 – 4.01) ²	178-179	272.4
17- α -ethinylestradiol (EE2) C ₂₀ H ₂₄ O ₂	11.3 @ 27°C ¹		3.67 (2.53 – 4.16) ²	182	296.4

¹ www.chemfinder.com

² LOGKOW© A databank of evaluated octanol-water partition coefficients (Log P)
<http://logkow.cisti.nrc.ca/logkow/display?OID=19500>

Many studies have reported E1, E2 and EE2 as EDCs with the strongest estrogenic effects (Snyder *et al.*, 1999; Snyder *et al.*, 2001; Tanaka *et al.*, 2001). These compounds consist of phenol rings that can interact with estrogen receptors and have extremely high biological potency even at low concentrations such as ng/L (Wen *et al.*, 2009). As humans and animals both excrete E1 and E2 via urine and feces, they can be found at high concentrations in municipal and agricultural waste-streams. Women can excrete 25 to 100 µg of E2 per day depending on the phase of the menstrual cycle (Okkerman and Groshart, 2001).

1.2. Ultraviolet (UV) Based Processes for Transforming EDCs

1.2.1. Ultraviolet (UV) Radiation in Water Treatment (Disinfection)

Ultraviolet (UV) lamps were first invented in 1901. By 1950's reliable UV disinfection facilities were demonstrated in Austria and Switzerland. In 1996 over 1000 small UV installations were made in Europe and in 2001 several large utilities adopted UV radiation as their primary disinfection mechanism. Hence UV technology has been in place for a number of years (IUVA/IOA, 2009). However, its popularity as a disinfection tool has rapidly increased since the early 2000s. Introduction of new regulations including Stage 2 Disinfectant/Disinfection Byproduct Rule (D/DBPR) and Long-term 2 Enhanced Surface Water Treatment Rule (LT2ESWTR) encourage the use of UV technology in drinking water treatment. Using UV can lower the formation of DBPs during the treatment process, and when coupled with chloramines the treated water leaving the plant will have disinfectant residual per SWTR

regulations. Higher log inactivation of *Cryptosporidium* and *Giardia* can be achieved at low cost with UV disinfection.

In the electromagnetic spectrum, UV wavelengths range from 100 nm to 400 nm, subdivided into four categories as shown below (USEPA 1999).

UV Type	Range (nm)
UV-A	315 – 400
UV-B	280 – 315
UV-C	200 – 280
Vacuum UV	100 – 200

Wavelengths between 245 and 285 nm produces optimum germicidal effects. Wavelengths in the germicidal range penetrate the cell walls of microorganisms and disrupt vital cell functions inhibiting reproduction, disabling induction of pathological effects or killing them altogether (EPA, 1999). Other advantages of UV disinfection include: no known toxic or significant nontoxic byproducts, no danger of overdosing, no effect on minerals in water, relatively simple installations; and low supervision, maintenance or space requirements. Due to these benefits, UV is also used in disinfection of wastewater, storm water and reuse waters (IUVA/IOA, 2009).

Types of UV lamps used for disinfection purposes include: low-pressure lamp (LP) which emits nearly monochromatic light with maximum energy output at a wavelength of 253.7 nm; medium pressure (MP) lamp with polychromatic emission spectra from 180 nm to 1370 nm and low pressure high output lamp (LPHO) that emit at other wavelengths in a high intensity “pulsed” manner (USEPA, 1999). These lamps consist of mercury atoms which upon collision produce UV light. Table 1.2 shows the characteristics of LP-, LPHO- and MP-UV lamps. Figure 1.2 shows emission spectra of

LP-UV and MP-UV compared to absorbance spectrum of DNA in cells of microorganisms.

Table 1.2 Typical mercury vapor lamp characteristics (USEPA, 2006)

Parameter	Low-pressure	Low-pressure High-output	Medium-pressure
Germicidal UV Light	Monochromatic at 254 nm	Monochromatic at 254 nm	Polychromatic, including germicidal range (200 – 300 nm)
Mercury Vapor Pressure (Pa)	Approximately 0.93 (1.35×10^{-4} psi)	0.18 – 1.6 (2.6×10^{-5} – 2.3×10^{-4} psi)	40,000 – 4,000,000 (5.80 – 580 psi)
Operating Temperature (°C)	Approximately 40	60 – 100	600 – 900
Electrical Input [watts per centimeter (W/cm)]	0.5	1.5 – 10	50 – 250
Germicidal UV Output (W/cm)	0.2	0.5 – 3.5	5 – 30
Electrical to Germicidal UV Conversion Efficiency (%)	35 – 38	30 – 35	10 – 20
Arc Length (cm)	10 – 150	10 – 150	5 – 120
Relative Number of Lamps Needed for a Given Dose	High	Intermediate	Low
Lifetime [hour (hr)]	8,000 – 10,000	8,000 – 12,000	4,000 – 8,000

Note: Information in this table was compiled from UV manufacturer data.

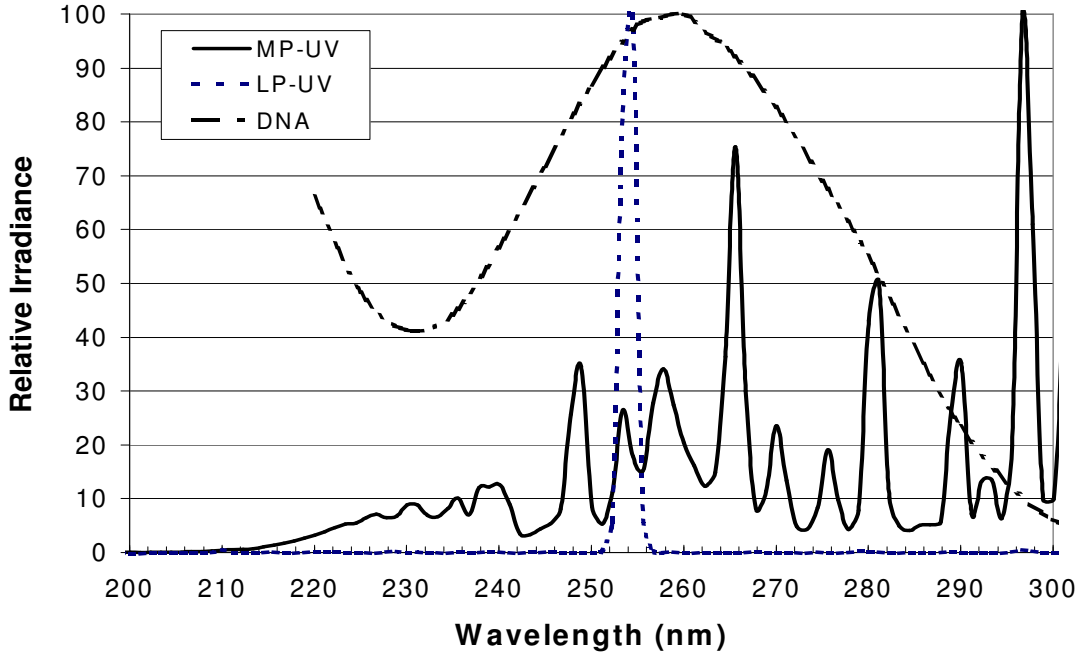


Figure 1.2 Relative Emission Spectra from Low (LP-UV) and Medium Pressure (MP-UV) UV Lamps as Compared to the Absorbance Spectrum of DNA (Sharpless, 2001)

UV Transmittance (UVT) is a parameter used in describing the behavior of UV light. UVT is the percentage of UV light passing through a media and it can be estimated using Beer's law (Equation 1.1) (USEPA, 2006):

$$\%UVT = 100 \times \frac{I}{I_0} \quad (1.1)$$

Where,

- UVT = UV transmittance at a specified wavelength and pathlength
- I = Intensity of light transmitted through the sample [milliwatt per centimeter squared (mW/cm^2)]
- I_0 = Intensity of light incident on the sample (mW/cm^2)

UVT is usually reported for 254 nm wavelength and 1 cm pathlength. In case a different pathlength is used, it should be specified or converted to UVT for a

pathlength of 1 cm. UVT can also be calculated in terms of UV absorbance (Equation 1.2) (USEPA 2006):

$$\%UVT = 100 \times 10^{-A} \quad (1.2)$$

Where,

UVT = UV transmittance at a specified wavelength and

A = UV absorbance at a specified wavelength and pathlength (unitless)

The UV dose delivered depends on the UV intensity, the flow rate and the UVT.

The UV dosage is calculated as:

$$D = I \bullet t \quad (1.3)$$

D = UV Dose (mW-s/cm²)

I = Intensity, (mW/ cm²)

t = Exposure time (s)

Thus, for a certain dose to be delivered, a sample can be irradiated with low intensity UV for a longer period of time or, high intensity UV for a shorter period of time. During disinfection, log inactivation of microorganism is directly proportional to the UV dose delivered. UV light must be absorbed by the target pathogens for their inactivation. The following Table 1.3 shows UV doses used for disinfection of several target pathogens (USEPA, 2006).

Table 1.3 Disinfection UV Dose requirements in millijoules per centimeter squared (mJ/cm²)¹

Target Pathogens	Log Inactivation							
	0.5	1.0	1.5	2.0	2.5	3.0	3.5	4.0
<i>Cryptosporidium</i>	1.6	2.5	3.9	5.8	8.5	12	15	22
<i>Giardia</i>	1.5	2.1	3.0	5.2	7.7	11	15	22
Virus	39	58	79	100	121	143	163	186

¹ 40 CFR 141.720(d)(1)

1.2.2. UV Photolysis for Chemical Treatment

When UV is used for transformation of chemicals including, taste and odor compounds like geosmin and methylisoborneol (MIB) (Rosenfeldt *et al.*, 2005) or trace contaminants like N-nitrosodimethylamine (NDMA) (Sharpless and Linden, 2003) and EDCs (Rosenfeldt and Linden, 2004), the amount of photolysis depends on the UV light absorbed by the targeted compounds. The amount of radiation absorbed by a compound is known as the molar absorption coefficient of that compound and is denoted by ϵ , with units of $M^{-1}cm^{-1}$. This parameter is wavelength specific and varies across UV spectrum for a compound as shown in Figure 1.3. The figure shows that E1, E2 and EE2 have high molar adsorption between 200 to 300 nm, with a minimum absorption at approximately 250 nm and negligible absorption beyond 300 nm. Thus, LP lamp which emits UV at approximately 254 nm may not be able to degrade these compounds as effectively as the MP lamp which emits multiple UV peaks between 200 and 300 nm (Figure 1.2). Therefore, the molar adsorption coefficients help in determining the type of UV source that would be most effective in degradation of the associated compounds.

Another factor dictating transformation of a compound via UV light is the quantum yield, denoted by Φ . The Quantum yield is a measure of the photon efficiency of a photochemical reaction. It signifies a number of moles of compound removed per mole of photon absorbed by the compound (Bolton and Stefan, 2002). The overall quantum yields describing MP UV photolysis of the trace contaminant examined in this study (E1, E2, and EE2) were 0.29, 0.10 and 0.06 mol/Es, respectively (Φ for E2 and EE2 from Rosenfeldt and Linden, 2004; Φ for E1 from Studer and Sharpless, unpublished data).

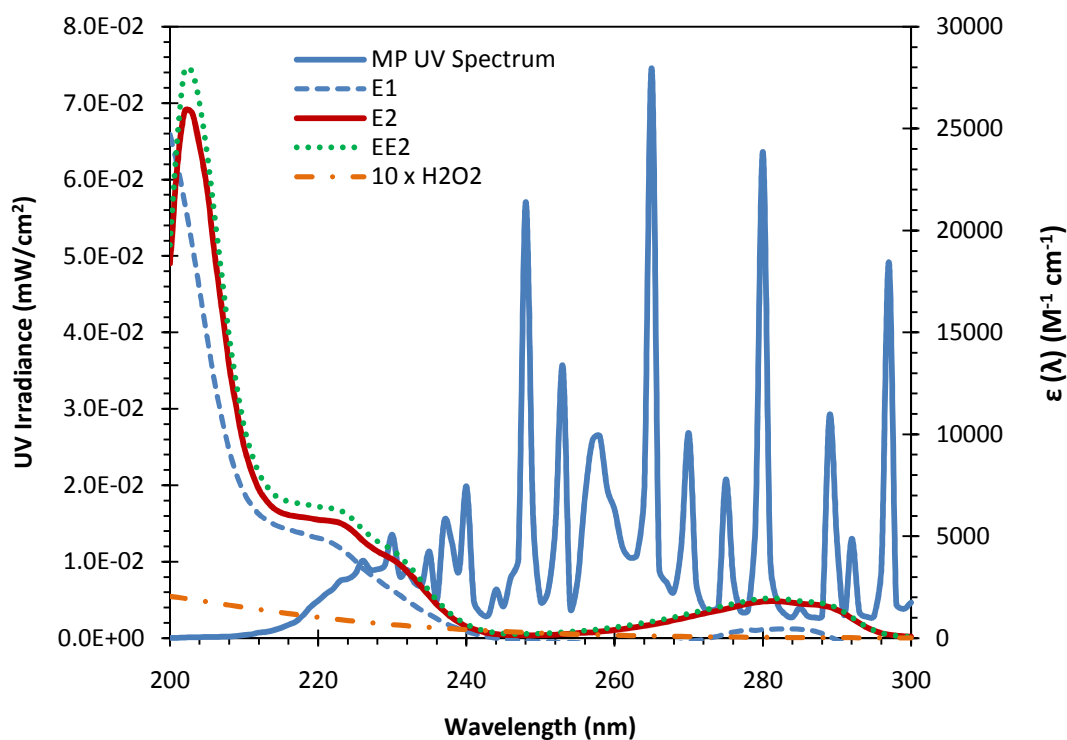


Figure 1.3 Absorption of E1 (from this study), E2, EE2, and H₂O₂ over the UV spectrum (UVC = 200-280nm, UVB = 280-315nm). The molar absorption coefficients of H₂O₂ have been multiplied by 10 to display them on the same graph (Based on Rosenfeldt and Linden, 2004).

1.2.3. UV Based Advanced Oxidation Process

In advanced oxidation process (AOP), an oxidizing intermediate species such as hydroxyl radical is generated which reacts with the target contaminant resulting in its oxidation. Various oxidants can be used to generate hydroxyl radical during the process. Some of the oxidants include peroxide (H_2O_2), ozone (O_3), oxygen (O_2) and titanium dioxide (TiO_2). In UV AOP applications, UV energy is absorbed by the listed oxidants resulting in the formation of hydroxyl radicals ($\cdot\text{OH}$). For example:



Where,

$h\nu$ = light source (UV)

During the specific process represented by Equation 1.4, only one hydroxyl radical is produced per molecule of reacting H_2O_2 , which is due to recombining effects during the process. Thus the quantum yield for the process is 1 mol of hydroxyl radical per Einstein absorbed by H_2O_2 (Rosenfeldt *et al.*, 2006). A combination of one or more oxidants with UV can be used during an advanced oxidation process. The possible combination includes: UV/ H_2O_2 , UV/ O_3 / H_2O_2 , and UV/ TiO_2 (SET, accessed February 2010; Rosenfeldt *et al.*, 2007). During UV photolysis, organic pollutants can directly absorb UV light and decompose. However, if the organic compounds are recalcitrant, UV photolysis alone may not be powerful enough to transform the desired amount of those compounds. In such case, addition of H_2O_2 will enhance the degradation of organic compounds due to the formation of highly reactive hydroxyl radicals which react with the pollutants.

AOPs can be used in removal of organic compounds. During AOP hydroxyl radical oxidizes organic contaminants to potentially less hazardous products with less handling issues. Thus, AOP treatment technology is gaining popularity in drinking water, wastewater, storm water and industrial water treatment. Some advantages and disadvantages of AOP over other contaminant removal technologies are as follows (SET, accessed February 2010):

Advantages of Advanced Oxidation Processes

- Rapid reaction rates
- Small foot print
- Potential to reduce toxicity
- Does not concentrate waste for further treatment with methods such as membranes
- Does not produce materials that require further treatment such as "spent carbon" from activated carbon absorption
- Does not create sludge as with physical chemical process or biological processes (wasted biological sludge)
- Non selective pathway allows for the treatment of multiple organics at once

Disadvantages of Advanced Oxidation Processes

- Capital Intensive
- High operating cost due to high expense associated with energy and H₂O₂
- Complex chemistry must be tailored to specific application

- For some applications quenching of excess peroxide is required

1.2.4. Removal of EDC activity with UV AOP

Studies have shown that UV photolysis and UV/H₂O₂ can transform EDCs and significantly reduce their estrogenic activity in water. A study revealed that MP UV can degrade estrogenic activity associated with EE2 by 95 % at UV fluence of 5000 mJ/cm² and 99% of the activity associated with E2 at 4000 mJ/cm². However, LP UV did not show reduction in estrogenic activity associated with either EE2 or E2 even at a fluence of 12000 mJ/cm² (Rosenfeldt *et al.*, 2007). When 5 mg/L of H₂O₂ was added both LP UV and MP UV were able to significantly reduce the estrogenic activity of EE2 and E2, although not at the same rate. Addition of H₂O₂ enhanced oxidation rate of E2 by 130 times compared to increase of EE2 destruction by 28 times (Rosenfeldt *et al.*, 2007).

Depending on water quality, various doses of UV had to be applied for 90% removal of estrogenic activity associated with 3 µg/L EE2. The applied UV dose ranged from 140 to 300 mJ/cm² in the presence of 5 mg/L of H₂O₂. The differences in required doses were attributed to the respective background scavenging present in the waters (Rosenfeldt *et al.*, 2007).

Similarly, in a study targeting the degradation of bisphenol A (BPA), UV/H₂O₂ showed effective removal of estrogenic activity to below detectable levels. UV alone was ineffective in degradation of BPA. However, due to high initial concentration of BPA used, the UV fluence applied were 50 -100 times higher than the does typically used during disinfection (Chen PJ *et al.*, 2006).

Rosenfeldt *et al.* (2007) found similarities between oxidation and estrogenic activity removal rates associated with E2 and EE2 during UV/H₂O₂ AOP, which implied non estrogen activity of the oxidation byproducts formed. Chen *et al.* (2006) also found degradation of the parent compound (BPA) and total estrogenic activity decreasing following UV/H₂O₂ AOP. However, their results suggested certain active metabolites may still be formed. They found in vivo estrogenic activity significantly lower than in vitro activity suggesting differences in sensitivities of the bioassays used.

All oxidation processes have not been deemed successful in removal of EDCs. Several studies have found increase in estrogenic activity following oxidation. Chlorinating BPA and 4-nonylphenol have found increase in the associated estrogenic activities as measured by; a yeast two-hybrid assay system (Hu *et al.*, 2002 a, b) and yeast estrogen screen (YES) (Lenz *et al.*, 2004). Thus, in addition to oxidation, adsorption processes have also been used in removal of organic contaminants from the environment.

1.3. Zeolite Media Adsorption

Traditionally activated carbon has been the adsorbent of choice for the removal of contaminants via adsorption process. While advanced oxidation process has been found effective in regenerating adsorption capacity of zeolites (Koryabkina *et al.*, 2007), oxidation of carbon surfaces, in general, have been known to significantly decrease the adsorption of phenol, nitrobenzene, benzene, and benzenesulfonate

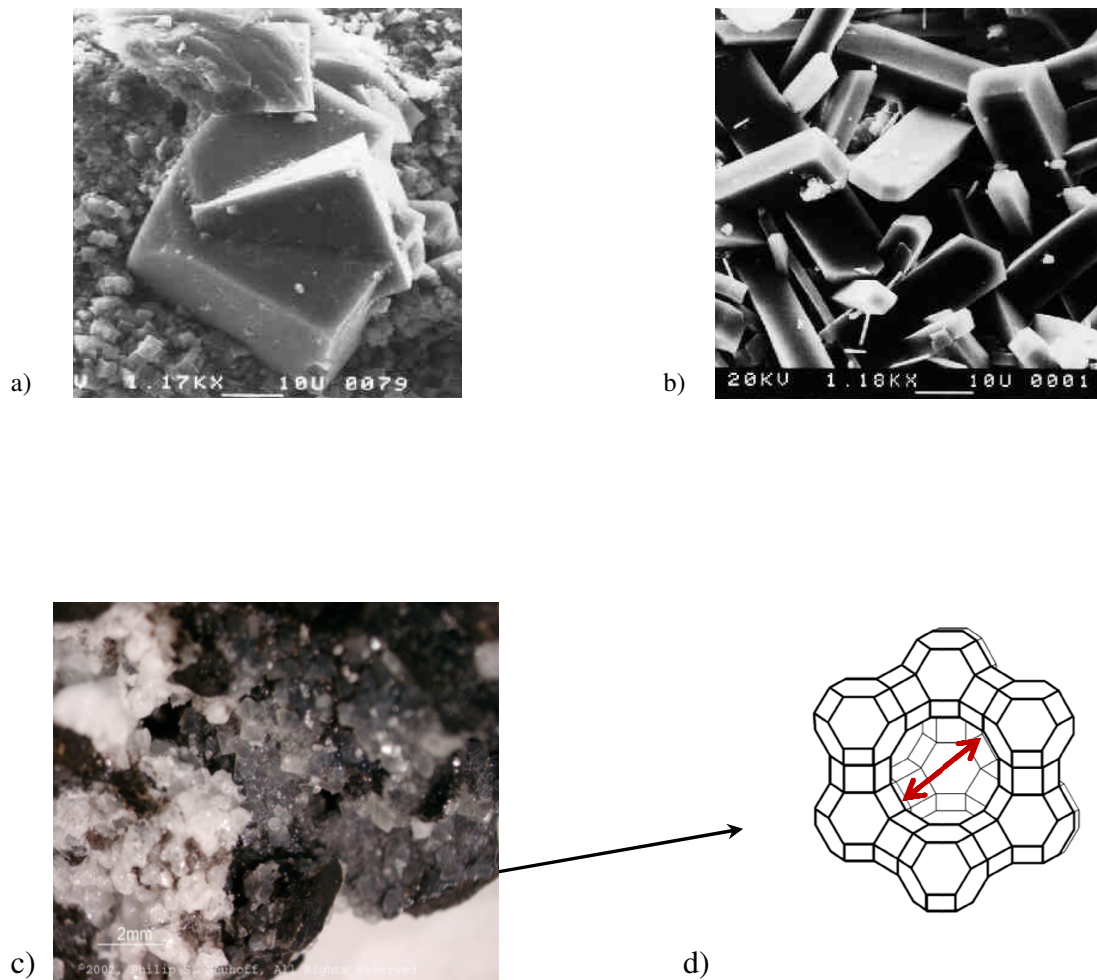
(Snoeyink and Summers 1999). Oxidation of the activated carbon surface with aqueous chlorine was also found to increase the number of oxygen surface functional groups and correspondingly to decrease the adsorption capacity for phenol. Thus, activated carbon can only be regenerated by mineralizing the adsorbed contaminants which requires extensive amount of heat (Snoeyink and Summers 1999), which is difficult and expensive. As a result, alternative media, such as inorganic materials, which can be regenerated multiple times at relatively low expenses, have been studied. Research has indicated that zeolites are a material which can easily be regenerated without disturbing their initial catalytic or adsorption properties (Khalid *et al.*, 2004).

1.3.1. Characteristics of Zeolites

Zeolites are already in use in industrial treatment processes. Y-type zeolites are the main adsorbent used in refining processes, specifically in fluid catalytic cracking during gasoline production (Marcilly, 2001). Zeolites have also been successfully investigated for adsorption of volatile organic compounds (VOCs, i.e., chloroform, trichloroethylene, tetrachloroethylene, carbon tetrachloride) (Giaya *et al.*, 2000) and EDCs (e.g. bisphenol A, estrone, etc.) (Tsai *et al.*, 2006; Wen *et al.*, 2009).

Zeolites are crystalline, porous alumino-silicates with well defined pore structures, and tetrahedral framework. Zeolites can be found naturally on earth's crust or can be manufactured. Figure 1.4 illustrates some of the natural zeolites available, and Table 1.4 shows some of the manufactured zeolite Y used in this study. Zeolite Y is a subset of faujasite. Primary building blocks of these zeolites are silica tetrahedra

and alumina tetrahedra which are illustrated in Figure 1.5. Zeolite Y has the sodalite cage structure shown in Figure 1.6 (Bhatia, 1990).



Note : Zeolite Photos Courtesy International Natural Zeolite Association

Figure 1.4 Natural zeolites: a) Chabazite; b) Clinoptilolite; c) Faujasite; d) tetrahedral framework found on Faujasite

Table 1.4 Properties of zeolites used as adsorbent.

Zeolite	Si/Al ratio	Unit Cell Size (Å)	Surface area (m ² /g)	Phase
CBV-400	2.6	24.52	817	Powder
CBV-780	40.5	24.24	861	Powder
CBV-901	41.3	24.2	743	Powder

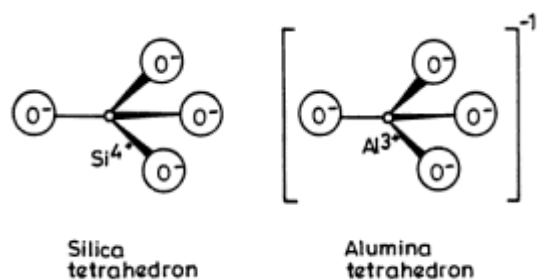


Figure 1.5 Primary building blocks of zeolites (Bhatia, 1990)

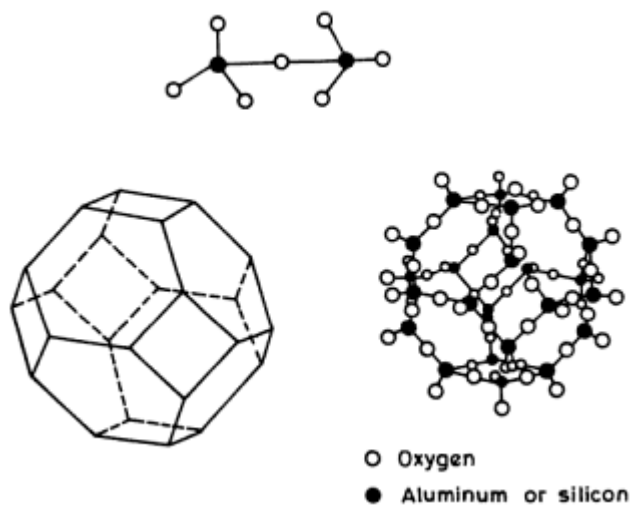


Figure 1.6 Sodalite cage structure (Bhatia, 1990)

Hydrophobicity of zeolites is characterized using the Si/Al ratio. The higher the Si/Al ratio, the more hydrophobic the zeolites are. To effectively absorb inorganic contaminants selectively from water, adsorbents must be hydrophobic and organophilic. Several studies have shown that adsorption of water vapor on zeolites decreases linearly with decreasing number of aluminum atoms per gram of zeolites. As a result, adsorption of organic compounds increases with increasing Si/Al ratio. When Si/Al ratio was increased from 5 to 100, adsorption of phenol molecules per supercage in zeolites increases from 0.17 to 0.81 (Khalid *et al.*, 2004). In the range of Si/Al ratio equal to 16 – 100, zeolite pore structures appeared to be a significant parameter in determining adsorption capacity. Zeolites with supercages and a three-dimensional structure seemed to perform better than other zeolites with similar adsorption capacities.

1.3.2. Zeolites for Removal of Organic Contaminants in Water

Studies have shown that zeolites can adsorb organic compounds rapidly. Khalid *et al.* (2004) found that the initial adsorption rate was rapid and a plateau was reached within 15 minutes. Similarly, Koryabkina *et al.* (2007) reported that adsorption of chloroform (CLF) on zeolites occurred rapidly as initial concentration of 30,000 mg/L reduced to an equilibrium concentration of 5000 µg/L within 15 minutes. Wen *et al.* (2009) found that adsorption equilibrium for dealuminated zeolite Y (DAY) was reached within 4 hours.

In the presence of water, hydrophobicity constituted the main parameter determining the competitive adsorption of organic compounds such as phenol, in a

study conducted by Khalid *et al.* (2004). In their study, faujasite appeared to be the most promising hydrophobic adsorbent. Reungoat *et al.*, (2007) also found faujasite as the zeolite with the highest adsorption capacity when investigating removal of nitrobenzene (NB) from water.

In Khalid's (2004) study, at higher phenol concentration, activated carbon proved to be more efficient than zeolite which was attributed to larger surface area, 1150 m²/g in activated carbon compared to 500 m²/g in the selected zeolite. On the other hand, at lower initial phenol concentrations, zeolite performed better than activated carbon due to differences in their pore sizes. Activated carbon has a wide range of pore sizes which makes it non size-selective. Thus phenol molecules can diffuse rapidly inside the activated carbon pores and can also desorb easily during the process. Whereas, in the case of zeolite, specifically sized channel structures would create confinement effect, limiting desorption (Khalid *et al.*, 2004).

Due to their relatively small and uniform pore sizes, zeolites are selective adsorbents. Additionally, their mineral composition makes them highly resistant to chemical agents including, acids, bases, and oxidants such as ozone (Reungoat *et al.*, 2007). Khalid *et al.* (2004) showed that zeolites were not sensitive in acidic solution. The adsorption capacity for a pollutant, phenol in this case, stayed constant for pH 4 and 6 (160 mg/g); while the capacity decreased (120 mg/g) when pH increased from 6 to 8.

1.3.3. Potential for Zeolite Regeneration

In order to increase the efficiency of zeolite-adsorption, various regeneration methods have been studied. Khalid *et al.* (2004) regenerated zeolite by completely oxidizing phenol into CO₂ and H₂O under air flow at 400 °C with a rate of increase of 2 °C/min. Using this method, zeolite was regenerated for 10 times demonstrating efficient regeneration and recycling of zeolite as adsorbent. Reungoat *et al.* (2007) regenerated zeolite via ozonation. During this process, if the conditions were favorable, the organic matter could completely mineralize. But often times, hydroxyl radicals are produced at lower concentrations leading to the formation of byproducts rather than complete mineralization of contaminants. The byproducts, in some cases, can be more hazardous to environmental and human health than the original compound (Reungoat *et al.*, 2007). Additionally, previous studies have found that organics adsorbed onto zeolites can be oxidized faster by ozonated water than those not adsorbed, because of a micropore concentration effect (Fujita *et al.*, 2004; Sagehashi *et al.*, 2005).

Advanced oxidation process has also been studied as regeneration mechanism for hydrophobic zeolites. A study used zeolites to adsorb disinfection byproducts (chloroform and trichloroacetic acid) and subsequently regenerated them via Fe⁰/H₂O₂ advanced oxidation process. After each adsorption event, zeolites were coated with Fe⁰ and subjected to advanced oxidation through addition of H₂O₂ which resulted in constant capacity for adsorption through 4 regeneration cycles (Koryabkina *et al.*, 2007).

Another study investigated UV photolysis at 254 nm for regeneration of zeolites with estrone (E1) adsorbed onto them. The method was found successful in regenerating the adsorption capacity of zeolites multiple times (Wen *et al.*, 2009). Other studies indicated that irradiation of estrone breaks and oxidize benzene rings resulting in products containing carbonyl groups which are considered to have negligible estrogenic activity due to lack of phenol rings (Ohko *et al.*, 2002; Liu and Liu, 2004).

2. INTRODUCTION

2.1. Problem Statement

In light of extensive literature review, oxidation and sorption were identified as potentially effective methods for the removal of unwanted compounds from waste stream. Each of these methods has its drawbacks. Oxidation processes can chemically transform compounds such that the products no longer contain the properties of parent compounds. However, this does not guarantee the mitigation of the problem in its entirety. Oxidation products may, in some cases, be more toxic or hazardous than the original compounds (Hu *et al.*, 2002 a, b; Lenz *et al.*, 2004). Full mineralization of EDCs to CO₂ and H₂O may be achieved but requires exorbitant UV treatment conditions which are often not feasible depending on the dynamics of the treatment train. Consequently, multiple unknown transformation products are typically formed with oxidation processes (Chen *et al.*, 2006).

Conversely, adsorption processes physically remove the contaminant from water but leave a “concentrated” waste stream with highly elevated levels of contaminants in the adsorbent. Careful consideration must be given to disposing such a concentrated stream so that it does not pose threats to environmental and human health. Disposal sites must be chosen cautiously so that the contaminant does not leach into ground water or surface water systems.

This study attempts to investigate a mechanism which can address both issues by adsorbing, then oxidizing the “concentrated” stream to minimize the impacts of trace contaminants, specifically EDCs in this case. Studies have found that organics adsorbed onto zeolites can be oxidized faster by ozonated water than those not

adsorbed, because of a micropore concentration effect (Fujita *et al.*, 2004; Sagehashi *et al.*, 2005). Additionally, oxidation of the adsorbed material may result in regeneration of the zeolite material and significantly increase the ultimate EDC adsorption capacity.

Several studies have shown that conventional wastewater treatment processes are inefficient in removing EDCs found in municipal or industrial waste water (Wells *et al.*, 2008; Chen PJ *et al.*, 2006; López de Alda and Barceló, 2001). As a result EDCs have been detected in surface water, ground water supplies or sewage effluent worldwide (Petrovic *et al.*, 2004). Thus, it makes the exploration of such mitigation techniques all the more critical in dealing with removal of hazardous materials such as EDCs from the environment.

2.2. Objectives

The three main objectives of this study were as follows:

1. Examine the fundamentals of adsorption of EDCs, specifically estrone (E1), 17- β -estradiol (E2) and 17- α -ethinylestradiol (EE2) on to three zeolites- CBV-400, -780 and -901 obtained from Zeolyst International.
2. Examine fundamental aspects affecting UV and the UV/H₂O₂ AOP for regeneration of the adsorption capacity of zeolites saturated with EDCs.
3. Examine the fundamentals of adsorption of EDCs onto selected zeolites and assess the effectiveness of the regeneration process in natural water conditions.

3. MATERIAL AND METHODS OF INVESTIGATION

3.1. Chemicals, Materials and Equipments

Tables 3.1 and 3.2 show a list of chemicals, materials and equipment used during the course of this study. Methanol was used for the preparation of standards for E1, E2 and EE2. Most of the chemicals including, E1, E2, EE2, methanol and acetonitrile were procured from Fisher Scientific.

Table 3.1 List of chemicals used in the study

Chemical	Use	Grade	Source
Methanol	Solvent	HPLC Grade, Also meets ACS Specifications 0.2 micron filtered	Fisher Scientific, USA
Acetonitrile	Eluent	HPLC Grade, Also meets ACS Specifications 0.2 micron filtered	Fisher Scientific, USA
Estrone	Adsorbate	---	Fisher Scientific (MP Biomedicals LLC), USA
17 β -estradiol (E2)	Adsorbate	---	Fisher Scientific (MP Biomedicals LLC), USA
17 α - ethinyl estradiol (EE2)	Adsorbate	---	Fisher Scientific (MP Biomedicals LLC), USA
Dealuminated Y (DAY) -CBV 400 -CBV 780 -CBV 901	Adsorbent	N/A	Zeolyst International, Conshohocken, PA USA
CaCl ₂	Desiccant	---	Sigma Aldrich, St. Louis, MO USA
H ₂ O ₂	Oxidant	30% (W/W) Aqueous Solution, ACS Reagent Grade	RICCA Chemical Company, Arlington, TX USA
Deionized Water	Solvent	---	Reverse Osmosis Pure Water System with Deionization/ Fluid Solutions, Lowell, MA USA
Natural Water	Solvent	N/A	Northampton, MA

Table 3.2 List of materials and equipments

Materials/Equipments		Use	Model/Make/Source
High Pressure Liquid Chromatography (HPLC) Unit		EDC Detection	Alliance Waters 2690 Separation Module, Milford, MA USA
HPLC Column		Chromatography Separation	Prevail Select C18 5 μ (4.6 mm \times 150 mm) –Grace Division Discovery Sciences, Deerfield, IL USA
Photo Diode Array (PDA)		EDC Detection	Waters TM 996, Milford, MA USA
Water Purification Unit			Millipore Milli-Q® Gradient, Billerica, MA USA
UV light	Low Pressure (LP)	Regeneration	Homemade
	Medium Pressure (MP)	Regeneration	Calgon Carbon Co., Pittsburg, PA
UVC Radiometer		Measurement	UVC 254, Mannix Testing & Measurement, Hewlett, NY
Spectroscopy System		Detection	Agilent 8453 UV-Visible, Agilent Technologies, USA
TN & TOC Analyzer		Detection	SHIMADZU: TOC-V _{CPH} , TNM-1, Columbia, MD USA
Inductively Coupled Plasma - Optical Emission Spectrometer (ICP-OES)		Cation Detection	Perkin Elmer/ Waltham, MA USA
Ion Chromatography (IC)		Anion Detection	CD25 Conductivity Detector, EG50 Eluent Generator, AS50 Autosampler/,GP50 Gradient Pump/ DIONEX
Centrifuge		Separation	Sorvall RC 5C Plus – DuPont, USA
Centrifuge Rotors		Separation	GS-3, SA-600
Centrifuge bottles/tubes		Separation	Fisher Scientific, USA
Crystallizing Dishes		Regeneration	KIMAX ® /Fisher Scientific, USA
Orbital Shaker		Mixing	G10 GYROTOR® Shaker, New Brunswick Scientific Co, Inc. Edison, NJ USA
Hot plate magnetic stirrer		Mixing	Fisher Scientific, USA
Magnetic Stirrer		Mixing	Thermix Stirrer Model 1205, Fisher Scientific USA
Membrane filter		Separation	Millex- HV, Hydrophilic PVDF 0.45 μ m, 25 mm, 47 mm/ Millipore, Billerica, MA USA
pH meter		pH	Fisher Scientific, USA
Desiccator		Desiccate	Boekel Phila Penna, Feastervl Trvs, PA
Oven		---	Isotemp Oven, Fisher Scientific, USA
Weighing Dishes (Aluminum and Plastic)		Weighing	Fisher Scientific, USA
Vacuum Pump		Filtration	GAST Manufacturing Inc, Benton Harbor, MI USA
Filter Apparatus		Filtration	Pall Gelman Sciences, Port Washington, NY

3.2. Experimental Design

Three main sets of experiments were conducted. The first set of experiments determined adsorption kinetics. The second set involved adsorption of EDCs on to zeolites in order to achieve equilibrium. The third set consisted of processes to regenerate spent zeolites such that additional mass of EDCs could be adsorbed. All experiments were performed at room temperature.

3.2.1. Water Samples

While preparing estrogen-spiked samples, the main concern was to achieve consistency in the concentration of stock solutions. A concentration was selected such that all estrogens stock solutions could have same initial concentration, which was ~1.5 mg/L for this study. It was important to have same concentration for all estrogens in order to be able to accurately compare adsorption.

In order to prepare stock solutions, E1, E2 and EE2 were added in excess in deionized (DI) water, for 10 hours or more, on a hotplate stirrer. Magnetic stirring and low heat were applied to facilitate dissolution. After 10 hours, the solution was brought to room temperature and filtered through Millipore Millex- HV Hydrophilic PVDF 0.45 μ m membrane filter using GAST vacuum pump and Pall Gelman filter apparatus to remove undissolved compound. The concentration of stock solution was measured via High Performance Liquid Chromatography (HPLC), diluted to 1.5 mg/L, and immediately used for experiments. For the preparation of HPLC standard calibration curves for each of E1, E2 and EE2, respective compounds were mixed in

methanol and diluted in water to achieve a range of concentrations. The methanol-estrogen solutions were stored at 4 °C when not in use.

3.2.2. Adsorbent

Dealuminated Y (DAY) zeolites obtained from Zeolyst International were used as adsorbents. Properties of zeolites used: CBV-400, CBV-780 and CBV-901 are listed in Table 1.4. The information provided by the suppliers on the zeolites used is shown in Appendix A. Higher Si/Al mole ratio indicates greater hydrophobicity. Thus, among three zeolites selected, CBV-400 was the least hydrophobic. CBV-901 had the lowest surface area of 743 m²/g, and CBV-780 had the largest surface area of 861 m²/g.

Zeolites samples were prepared by drying them in an oven at 120 °C for 12 – 14 hours and then desiccating them in the presence of supersaturated solution of CaCl₂ in water in order to obtain moisture equilibrium (Wen *et al.*, 2009).

3.2.3. Adsorption Equilibrium

Adsorption isotherms were developed using a batch equilibrium technique to compare adsorption capacities of zeolites: CBV-400, -780 and -901 for estrogens. Various masses of zeolites were immersed in aqueous estrogen solutions and left overnight on an orbital shaker at approximately 275 RPM to equilibrate in ambient conditions.

For this study zeolite concentrations ranged from 10 to 200 mg/L. Sample volumes were varied in order to attain the target zeolite concentrations for

equilibrium experiments. Table 3.3 shows some of the typical liquid volumes and zeolite masses used to attain target zeolite concentrations.

Table 3.3 Typical zeolites concentration used for adsorption equilibrium experiments

Sample Volume (mL)	Zeolite mass (mg)	Zeolite Concentration (mg/L)
500	5.0	10
500	7.5	15
500	10.0	20
500	14.0	28
500	18.0	36
500	22.0	44
500	28.0	56
250	16.0	64
250	18.0	72
250	22.0	88
250	24.0	96
125	13.0	104
125	14.0	112
125	15.0	120
125	17.0	136
125	19.0	152
125	25.0	200

3.2.4. Adsorption Kinetics

Since zeolite CBV-400 showed minimal adsorption capacity for estrogens, kinetics experiments were conducted only with CBV-780 and -901. For each zeolite, a concentration was selected such that if given enough time, more than 90% reduction in estrogen concentration from its starting concentration could be achieved. From initial adsorption equilibrium experiments, the zeolite concentration which could achieve such reduction appeared to be 45 mg/L. At 45 mg/L CBV-780 could adsorb 90% or more, while, CBV-901 could adsorb 95% or more of estrogens from the aqueous solution. For these experiments sample volume of 125 mL was selected with zeolite mass of 5.5 to 5.7 mg. The initial concentration of estrogens was approximately 1.5 mg/L.

Sample collection times selected for kinetics experiments were 10, 20, 30, 45, 60, 90 and 120 minutes. These experiments were also performed in batch reactor fashion where separate samples, with replicates, were allocated for each time. All samples were placed on an orbital shaker at approximately 275 RPM throughout the selected reaction times.

3.2.5. Zeolite Media Regeneration

Figure 3.1 summarizes the process conducted to regenerate zeolite media for additional adsorption of estrogens. Two different treatments and a control setup were used during the regeneration process. The first treatment was UV photolysis and the second treatment was advanced oxidation process with UV and H_2O_2 . The control setup had same conditions as the other two treatments, except the zeolite media was not exposed to UV radiation and no H_2O_2 was added.

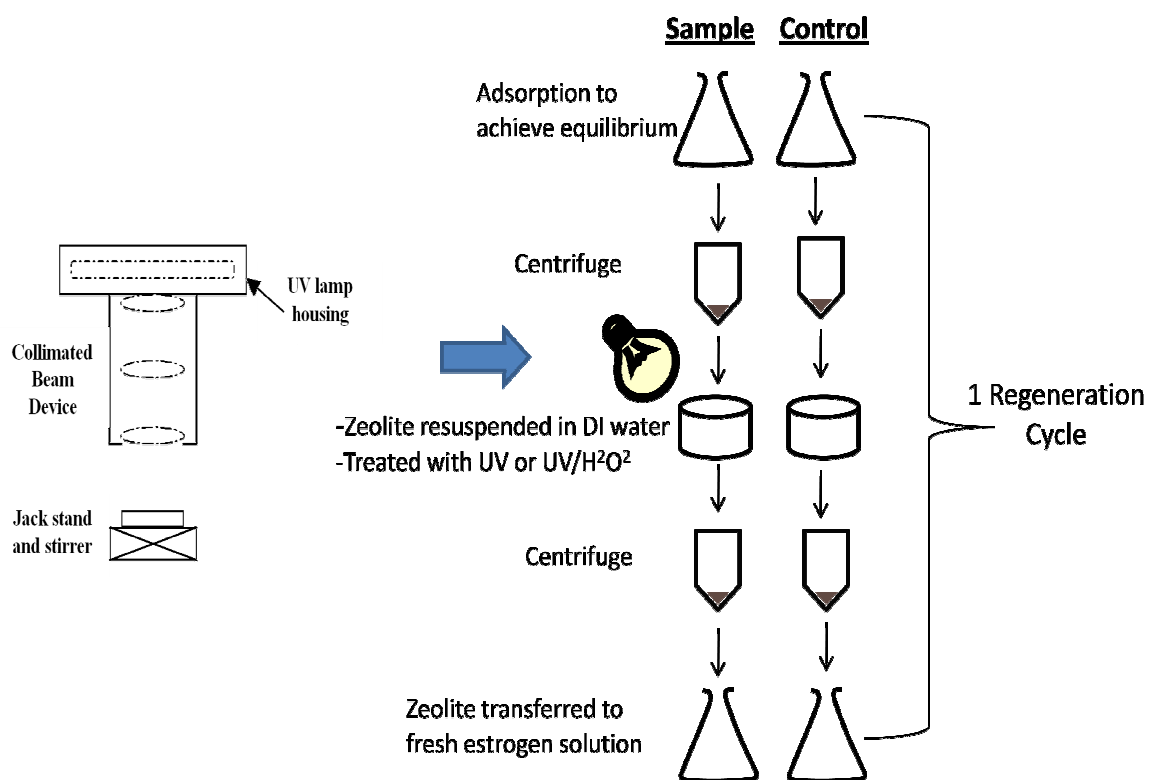


Figure 3.1 Regeneration of zeolites

The zeolite selected for the regeneration processes was CBV-780 which had slightly lower adsorption capacity than CBV-901 but proved to be the better of the two zeolites in revealing the regenerative capacity. Regeneration experiments were performed to investigate regeneration of CBV-780 in the presence of all three estrogens.

Based on the results from kinetics of reaction, at first, fresh zeolite was mixed in estrogen stock solution and allowed to equilibrate for an hour. The sample volume selected for regeneration processes was 800 mL, which was constrained by the centrifuge-apparatus available. The concentration of zeolite selected for this purpose was 40 mg/L. The initial concentration of E1 or E2 or EE2 in the stock solution was approximately 1.5 mg/L.

After mixing for 1 hour on an orbital shaker, zeolites were separated using a Sorvall RC 5C Plus – DuPont centrifuge unit. Based on the rotor used, centrifugation was carried out at 9000 RPM with selected temperature range of 2 – 4 °C. These conditions ensured minimal loss during transfer of zeolites between regeneration steps. The zeolites retrieved via centrifugation were transferred into a KIMAX® crystallizing dishes and were suspended in 100 mL deionized water. Subsequently, the zeolites were irradiated with MP UV radiation.

Following UV photolysis or UV AOP, the samples were once again subjected to centrifugation. The retrieved regenerated zeolites were re-suspended in fresh batch of estrogen stock solution and allowed to equilibrate for an hour on an orbital shaker. The duration between these adsorption equilibrium steps was termed as one regeneration cycle as illustrated by Figure 3.1. In total, 4 regeneration cycles were

performed. At the end of the last regeneration cycle, the zeolites were dried overnight in 100 °C oven, desiccated with supersaturated solution of CaCl_2 until equilibrium saturation, and weighed to assess the zeolite mass recovery through the entire process of regeneration.

More regeneration experiments were carried out with lower UV doses to examine the difference in regeneration capacity as UV radiation reduces. Both UV photolysis and UV/ H_2O_2 AOP were carried out at a lower UV dose. The main objective of performing these experiments was to find out if relatively high adsorption capacity of zeolites could be restored even at low doses of UV; and to ensure that excessive amount of UV was not being used for the process. This was important because lower UV doses correspond to lower operating costs which has a significant impact on the overall cost of the project when conducted on a large scale.

Another objective of varying UV doses was to examine if addition of H_2O_2 at lower UV doses could potentially contribute more in regenerating adsorption capacity of zeolites than at higher doses of UV. The irradiation times selected for these purposes were 5 and 15 minutes.

3.2.6. UV Irradiation Procedure

The MP UV used for the regeneration process utilized a 1 kW medium pressure Hg lamp housed in a bench-scale UV reactor (Appendix B). The reactor consists of a pneumatic shutter which was controlled with an automatic switch, preset to desired UV exposure time. House air was channeled to operate pneumatic shutter.

The UV exposure times selected for the process were 5, 15 and 30 minutes. All three EDCs: E1, E2 and EE2, when in dissolved state in DI, showed close to complete degradation within 30 minutes of MP UV photolysis (Appendix C). Radiometer measurements were taken before and after irradiation of sample to ensure consistency in UV dose throughout the regeneration process.

During irradiation the zeolite solution was continuously stirred with a magnetic stirrer to achieve uniform exposure of zeolite particles to UV radiation. In the second treatment, the zeolite solution was spiked with 10 mg/L of H₂O₂ prior to UV irradiation to generate an advance oxidation process. For the control setup, the solution was stirred in dark for the equal amount of time as the samples were exposed to radiation in the other two treatments.

3.3. Adsorption and Regeneration in Estrogen Spiked Natural Waters

After quantifying and restoring adsorption capacity of zeolites for the selected EDCs in deionized water, further investigation was done to examine how these processes could vary in natural water matrix. For this purpose, natural water samples were collected at two different locations along the treatment train in Northampton Water Treatment Plant (Northampton, MA). One sample was raw water, collected at the head of the plant. Another sample was post-filter water which had already been treated through coagulation, flocculation and filtration.

Both raw water and post-filter water were filtered through 0.45 µm filter disc to remove residual particulate matter. Prior to spiking the water with estrogen, water

quality parameters of both the samples were determined. The parameters investigated included: cations (Na, K, Mg, Ca and Fe), anions (chloride, sulfate, nitrate and phosphate), organic and inorganic carbon, and total nitrogen.

The estrogen selected for the experiments in natural water was E2 and the zeolite chosen was CBV-780. All the procedures and conditions applied to the experiments with natural water were same as those used in investigations with deionized water.

3.4. Analytical Methods

Acetonitrile was used as eluent for the analysis of aqueous estrogen samples in HPLC unit (Table 3.2). A photodiode array (PDA) was used for the detection of samples between 200 to 400 nm. Samples were analyzed at wavelengths of 205 nm and 222 nm. These two wavelengths were selected based on the adsorption spectra of E1, E2 and EE2 measured using the spectroscopy system listed in Table 3.2. The sensitivity of the detection at these wavelengths was higher compared to other wavelengths. Hence, as low a concentration as 9 µg/L of EE2 was detected.

A reverse phase, C-18 HPLC column (Table 3.2) was used for the separation of samples. For each estrogen, retention window of 10.5 minutes, with 1.5 minutes lag time between injections was selected. With eluent consisting 1:1 ratio of acetonitrile and ultra pure water from Millipore unit, average retention times for E1, E2 and EE2 were 8.4, 7.5, 8.7 minutes, respectively.

Sample flow rate through the column was 1 mL/min at pressure less than 1000 psi. In order to obtain precise data, three injections per sample, each injection of 100 µL

volume, were analyzed. All samples were analyzed at ambient temperature, which was approximately 22 °C. The calibration curves for E1, E2 and EE2 are included in Appendix D. All the calibration curves showed the best fit line with high correlation coefficients, R^2 values.

4. RESULTS AND DISCUSSIONS

Initially, adsorption of EDCs on all three zeolites was tested. Figure 4.1 illustrates adsorption of EE2 with increasing concentration of the zeolites. Similar results were observed for E2 and E1. CBV-400 showed poor adsorption capacity for all target estrogens. As seen in Figure 4.1, a high concentration of 90 mg/L of CBV-400 reduced EE2 concentration from 1.51 mg/L to 1.37 mg/L, achieving less than 10% reduction. Whereas, 40 mg/L of CBV-780 and 20 mg/L of CBV-901 reduced the initial concentration of EE2 by greater than 90%. Thus, CBV-400 was screened out from further investigations.

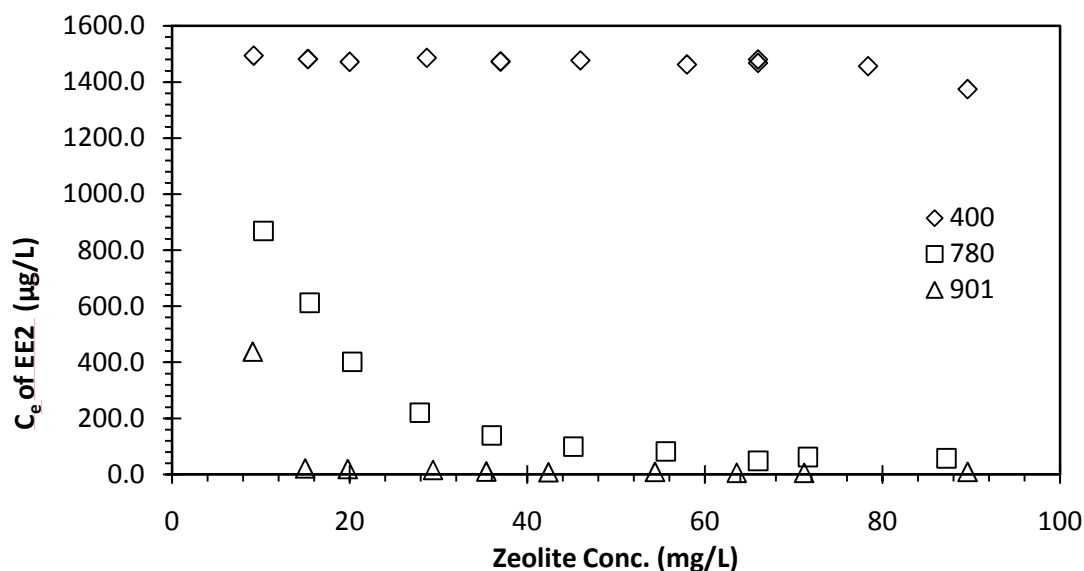


Figure 4.1 Adsorption of EE2 on all three zeolites, CBV-400, -780 and -901

The relative lack of adsorption capacity of CBV-400 can be explained by the Si/Al mole ratio in their molecular structures. As previously stated, the higher the Si/Al mole ratio, the greater the adsorption capacity. Among four zeolites tested, Khalid *et al.* (2004) found that at higher contaminant concentration, adsorption

capacity for phenol followed the Si/Al mole ratio. Increasing Si/Al ratio makes a zeolite more hydrophobic (Reungoat *et al.*, 2007; Khalid *et al.*, 2004). As shown in Table 1.4 CBV-780 and -901, both had higher Si/Al ratios of 40.5 and 41.3, respectively, while CBV-400 had the Si/Al ratio of only 2.6. Therefore, CBV-400 was the least hydrophobic zeolite, and thus less likely to be amenable to adsorption of contaminants. A study conducted by Khalid *et al.* (2004) indicated that on hydrophilic zeolites, water molecules can also compete with the organic contaminants for adsorption sites. He noticed that, the number of water molecules adsorbed to a hydrophilic zeolite supercage was 15 times more than the number of phenol molecules at a certain concentration.

4.1. Kinetics of Adsorption

Figures 4.2 through 4.4 illustrate the kinetics of reaction for the reduction of E1, E2 and EE2, respectively. The initial concentrations of E1, E2 and EE2 stock solutions were 1.41, 1.42 and 1.50 mg/L. Within 10 minutes, E1 was reduced to 90 µg/L by CBV-780 and 40 µg/L by CBV-901, reduction of >95% in each case.

Similarly, in the first 10 minutes of the reaction time, 1420 µg/L of E2 was reduced to 120 and 15 µg/L by CBV-780 and -901, achieving 90% and 99% reduction, respectively (Figure 4.3). Likewise, CBV-780 and -901 reduced 1500 µg/L of EE2 to 100 and 13 µg/L, achieving 93% and 99%, respectively in 10 minutes (Figure 4.4).

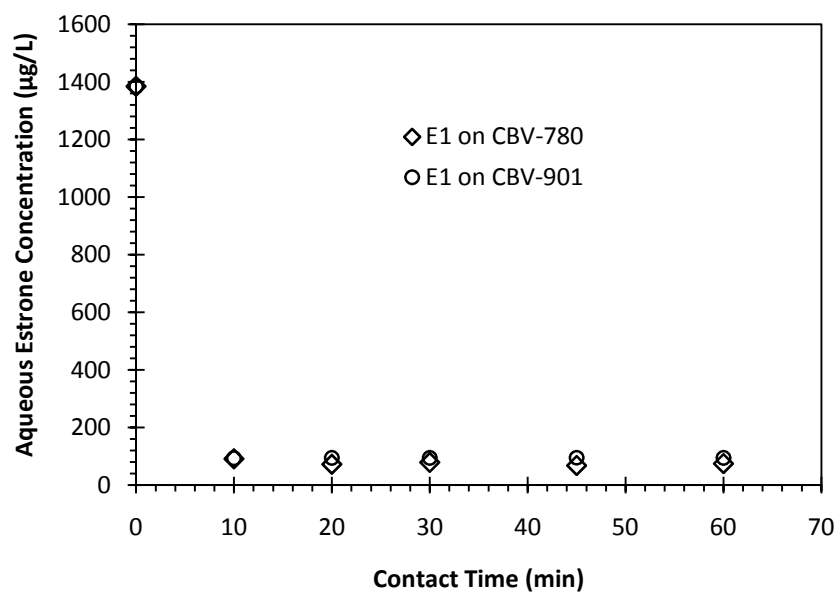


Figure 4.2 Kinetics of reaction for the adsorption of E1 on CBV-780 and -901

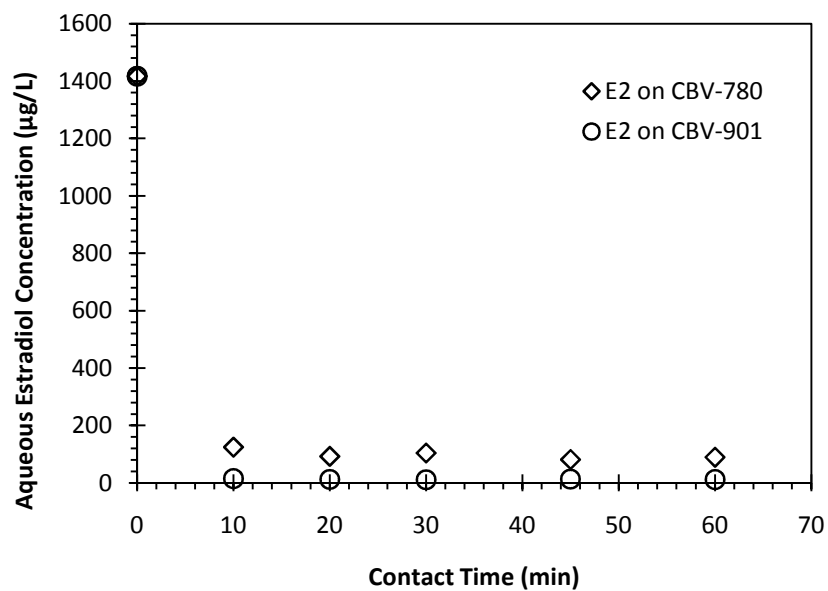


Figure 4.3 Kinetics of reaction for the adsorption of E2 on CBV-780 and -901

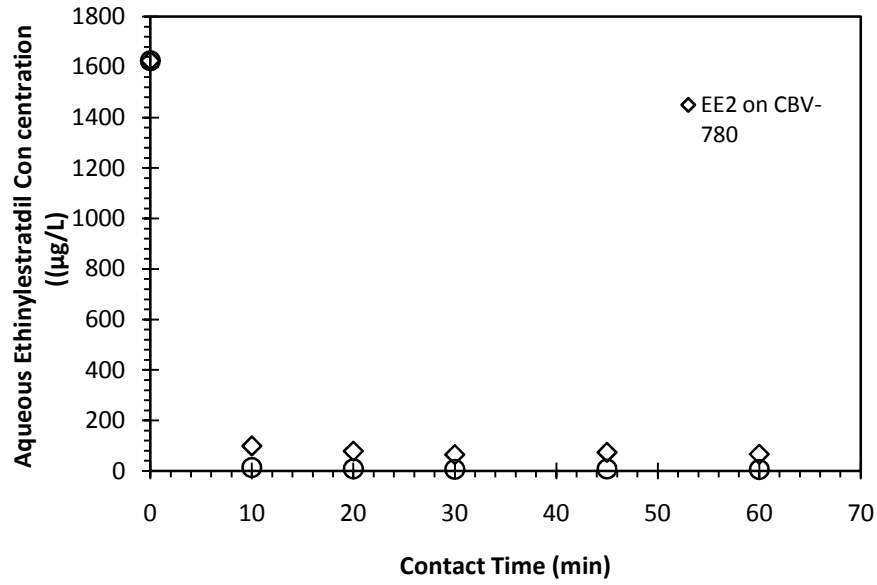


Figure 4.4 Kinetics of reaction for the adsorption of EE2 on CBV-780 and -901

4.2. Adsorption Equilibrium

Adsorption isotherms are generally nonlinear. In aqueous phase, Freundlich and linear models seem to better fit the adsorption data than models including, Langmuir, BET and Gibbs. However, at low adsorbate concentration, all the models approach linear model (Delle Site, 2001).

In an adsorption system q_{max} denotes adsorption capacity which represents the ratio of the mass of adsorbate to the unit mass of adsorbent. The maximum adsorption capacity is given by $q_{max} \cdot m$, where m equals the mass of the adsorbent. The kinetics of adsorption is given by equation 4.1 (Delle Site, 2001).

$$\frac{dc}{dt} = -k_1 \cdot m \cdot C(q_{max} - q) + k_2 \cdot q \cdot m \quad (4.1)$$

Where,

- q = concentration of the adsorbate in the solid phase (mg/g)
 m = mass of adsorbent (g)
 C = aqueous concentration of the chemical C (mg/L)
 k_1 = rate constant for adsorption
 k_2 = rate constant for desorption

Equation 4.1 shows that the rate of adsorption is proportional to the aqueous concentration of the chemical C and to the difference between the maximum capacity, $q_{max} \cdot m$, and the amount adsorbed, $q \cdot m$. At equilibrium, equation 4.1 reduces to the Langmuir isotherm shown in equation 4.2 where $b = k_1 / k_2$.

4.2.1. The Langmuir Isotherm

The non-linear Langmuir isotherm model is described with equation 4.2, and the linearized form is given by equation 4.3 (Snoeyink and Summers 1999).

$$q_e = \frac{q_{max} \cdot b \cdot C_e}{1 + b \cdot C_e} \quad (4.2)$$

$$\frac{1}{q_e} = \left(\frac{1}{b \cdot q_{max}} \right) \frac{1}{C_e} + \frac{1}{q_{max}} \quad (4.3)$$

Where,

- q_e = equilibrium surface concentration, measured as mass or moles of adsorbate adsorbed per unit mass of adsorbent (mg/g)
 q_{max} = surface concentration at monolayer coverage (mg/g)
 C_e = Equilibrium solution concentration, measured as mass or moles per volume (mg/L)
 b = energy of adsorption, increasing with adsorption strength.

Three important assumptions of the Langmuir model are: (1) the energy of adsorption is the same for all sites and is independent of degree of surface coverage,

(2) adsorption occurs only on localized “sites,” with no interaction between adjoining sorbed molecules, and (3) the adsorption maximum, q_{max} , represent monolayer coverage (Delle Site, 2001). Assumption (1) suggests homogenous surface which applies to zeolites CBV-780 and -901 as they have been manufactured to have specified surface areas, pore volumes and pore diameters. When the adsorbent surface is heterogeneous, the Langmuir equation is not generally considered to describe adsorption data as accurately as the Freundlich equation. In such cases, the experimentally determined values of q_{max} and b often are not constant over the concentration range of interest. Besides possible heterogeneous adsorbent surfaces, variation in q_{max} and b values has been attributed to factors including, lateral interactions between adsorbed molecules, which were neglected in the development of Langmuir model (Snoeyink and Summers 1999).

4.2.2. The Freundlich Isotherm

Another isotherm model considered for the data analysis was the Freundlich isotherm. When adsorbents are complex, the Freundlich-type isotherms can result from the overlapping patterns of several Langmuir-type sorption phenomena occurring at different sites with different interaction energies (Delle Site, 2001). The nonlinear Freundlich isotherm is shown in equation 4.4 and the linearized form is shown in equation 4.5.

$$q_e = K \cdot C_e^{1/n} \quad (4.4)$$

$$\ln q_e = \ln K_F + \frac{1}{n} \ln C_e \quad (4.5)$$

Where,

q_e = equilibrium surface concentration, measured as mass or moles of adsorbate adsorbed per unit mass of adsorbent (mg/g)

K_F = Capacity of the adsorbent for the adsorbate

C_e = Equilibrium solution concentration, measured as mass or moles per volume (mg/L)

$1/n$ = Function of both the relative magnitude and diversity of the energies (Delle Site, 2001)

For many compounds, the adsorption process is reversible. Adsorbate molecules continue to accumulate on the adsorbent until equilibrium conditions are achieved. At equilibrium, the rate of forward reaction i.e. sorption equals the rate of the reverse reaction i.e. desorption. The aqueous concentration of compound attained at equilibrium condition is known as equilibrium concentration which is denoted by C_e . The greater the K_F value, the larger the adsorption capacity. Whereas, the smaller the $1/n$ value, the stronger the adsorption bond between adsorbate and adsorbent.

Various types of chemical forces such as hydrogen bonds, dipole-dipole interactions, and van der Waals forces can exist between adsorbate and adsorbent (Snoeyink and Summers 1999). Figure 4.5 illustrates typical Freundlich isotherm models generated for various ranges of $1/n$ values.

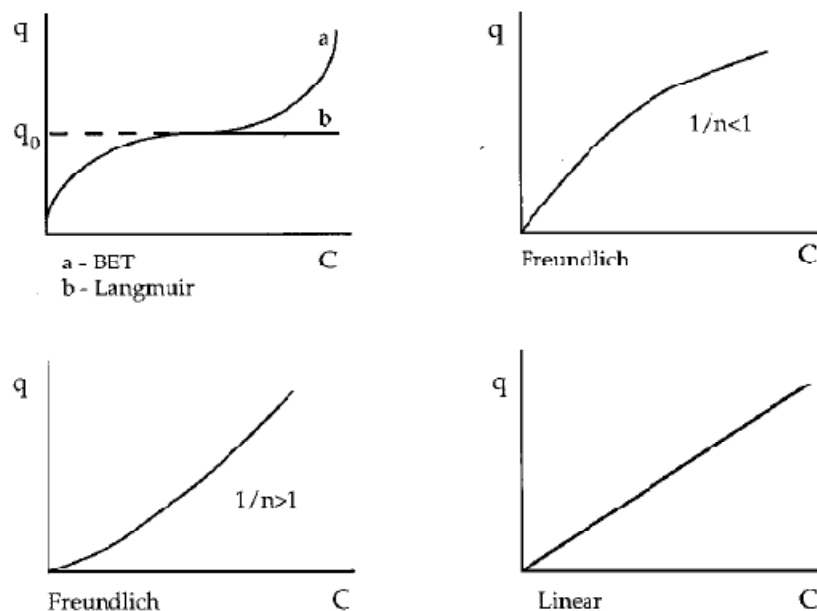


Figure 4.5 Typical isotherms describing sorption of organic compounds in water and vapor phase (BET) by natural sorbents (Delle Site, 2001).

A value of $1/n = 1$ suggests linear adsorption and equal adsorption energies for all sites. Linear adsorption occurs at very low adsorbate concentrations and low loading of the sorbent. A $1/n > 1$ generates a concave, curving upward isotherm, where the marginal adsorption energy increases with increasing surface concentrations. It can also imply strong adsorption of the solvent, strong intermolecular attraction within the adsorbent layers, penetration of the solute in the adsorbent, and monofunctional nature of the adsorbate. Such concave-type isotherms are more common for the soil fine fractions, which have a higher total amount of associated organic matter, than for the coarse fractions. A $1/n < 1$ generates a convex, curving downward isotherm, where the marginal sorption energy decreases with increasing surface concentration. Such phenomenon occurs where the competition of the solvent for sites is minimum or the adsorbate is a planar molecule (Delle Site, 2001).

4.2.3. Adsorption of the estrogens on the zeolite CBV-780

Figure 4.6 illustrates the nonlinear adsorption isotherms of E1, E2 and EE2. It shows increasing values of q_e with increasing equilibrium concentration, C_e .

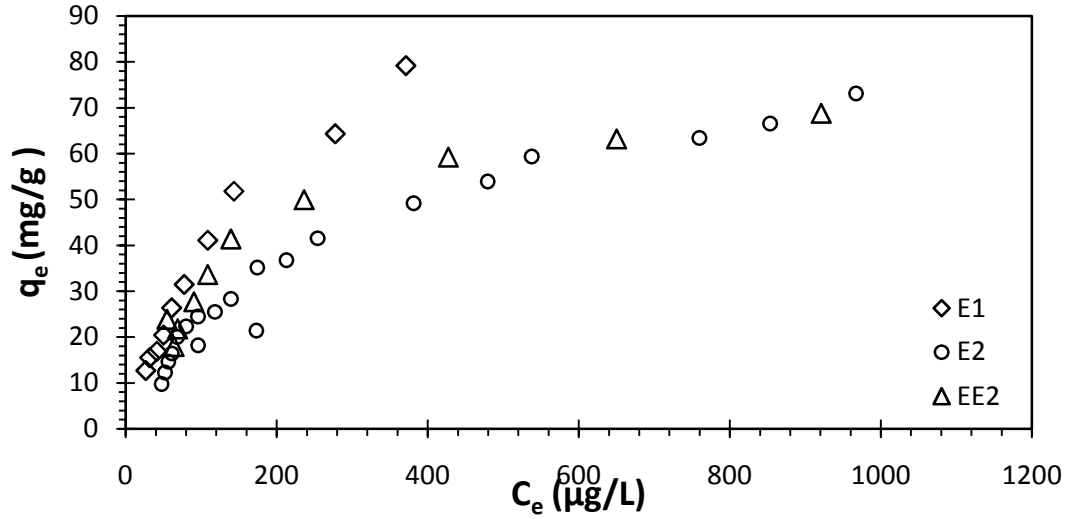


Figure 4.6 Adsorption isotherms of E1, E2 and EE2 on CBV-780

The data shown in Figure 4.6 were fitted in the linearized Freundlich and Langmuir adsorption models shown in Figures 4.7 and 4.8, respectively. As suggested by the high correlation coefficients R^2 values shown in the figures, both the Freundlich and Langmuir appeared to be appropriate isotherm models for the data obtained.

A q_{max} value, which suggests a maximum amount of adsorbate an adsorbent can hold, can be determined from linearized Langmuir model shown in Figure 4.8. This value can be checked against the experimental data shown in Figure 4.6. In the nonlinear isotherm plot, the q_{max} value for a given adsorbate-adsorbent combination is the q_e value where the data set plateaus.

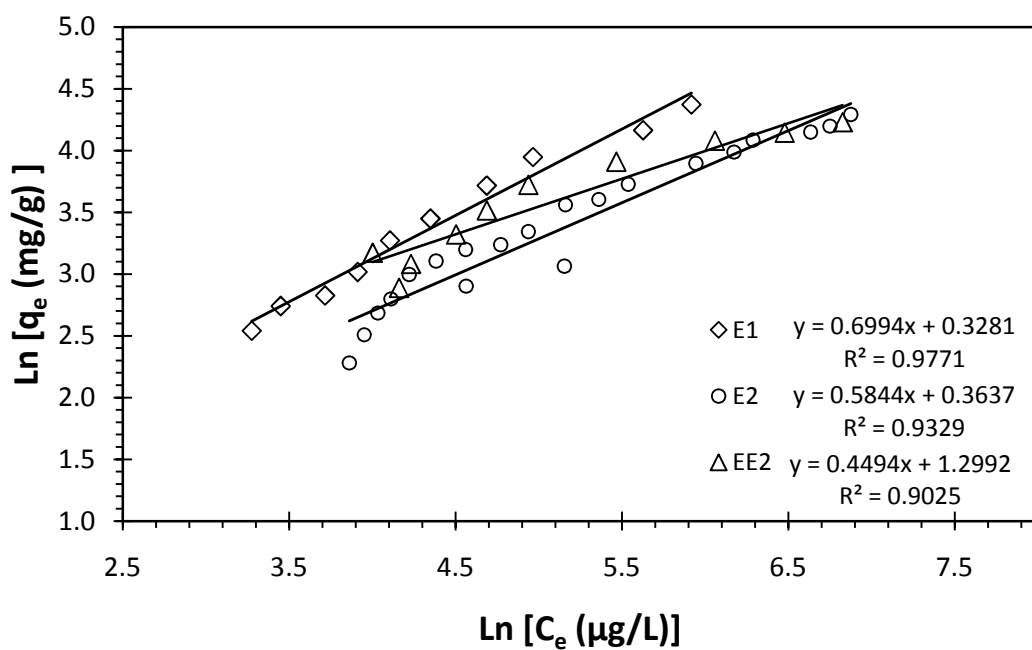


Figure 4.7 The linearized Freundlich isotherms of E1, E2 and EE2 on CBV-780

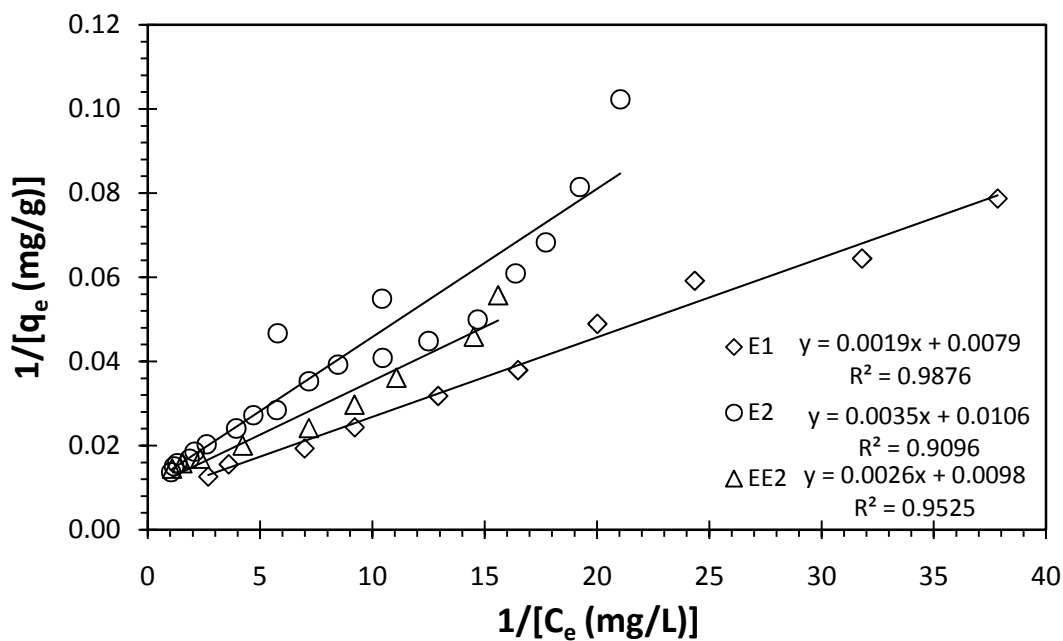


Figure 4.8 The linearized Langmuir isotherms of E1, E2 and EE2 on CBV-780

A summary of the Freundlich and Langmuir parameters are given in Table 4.1. The table shows that CBV-780 had the lowest q_{max} value for E2, followed by EE2 and E1. This does not agree with the Log K_{ow} values- 3.13, 4.01 and 3.67 of E1, E2 and EE2, respectively, reported by Hanselman *et al.* (2003), Lai *et al.* (2000) and recommended by LOGKOW© (accessed April 2010). The higher the Log K_{ow} , the more hydrophobic the compound is and consequently the more adsorbable the compound should be when in aqueous solution (Yoon *et al.*, 2003; Liu and Qian, 1995; Poerschmann *et al.*, 2000; Rao and Asolekar, 2001). However, ranges of Log K_{ow} values: 3.13 – 3.4, 3.57 – 4.01 and 2.53 – 4.16, have been reported by various researchers for aqueous phase E1, E2 and EE2, respectively (LOGKOW©, accessed in April, 2010). As the range of the Log K_{ow} values of E1, E2 and EE2 overlap their loading onto zeolite CBV-780 may not strictly follow the recommended Log K_{ow} values which suggests E2 as the most hydrophobic compound, followed by EE2 and then E1.

Table 4.1 Summary of adsorption isotherm parameters for CBV-780

Zeolite	EDC	Langmuir Parameters		Freundlich Parameters	
		q_{max} (mg/g)	b (L/g)	$1/n$	K_F [(mg/g)•(L/μg) ^{1/n}]
CBV-780	E1 (1.21 mg/L)	127	4.16	0.699	1.39
	E2 (1.63 mg/L)	94	3.03	0.584	1.44
	EE2 (1.63mg/L)	102	3.77	0.449	3.67
	EE2 (6.24 mg/L)	145	1.97	0.259	16.0

According to the Langmuir model, CBV-780 has the highest capacity of 127 mg/g for E1. The q_{max} values of EE2 and E2 were 102 and 94 mg/g, respectively. However,

the Freundlich parameter, K_F , which is also indicative of the adsorption capacity, was higher for EE2 (3.67) than for E1 (1.39), which agreed with the recommended Log K_{ow} .

The slopes of the linear trends of Freundlich isotherms shown in Figure 4.7 are equal to $1/n$ values (Table 4.1), and are indicative of how strongly E1, E2 and EE2 attach to zeolite CBV-780. E1 has the largest, and EE2 has the smallest slope and hence the respective $1/n$ values. The $1/n$ values indicated EE2 adsorbed most strongly to the zeolite, followed by E2, then E1.

During Molecular Dynamics simulations of a single E1 molecule in a DAY cavity, Wen *et al.* (2009) found that hydrogen atom in the –OH group formed a hydrogen bond with the oxygen atoms in the DAY structure, anchoring it to the cavity. The molecular structures, shown in Figure 1.1 indicate E1 has only one hydroxyl group, while E2 and EE2 each have two hydroxyl groups. Because of this, they may adsorb more strongly to the DAY structure, explaining the lower $1/n$ values, 0.584 (E2) and 0.499 (EE2) observed than for the E1 case (0.699). However, the regression analysis with 95% confidence interval for $1/n$ values further confirmed that adsorptive energy for all three estrogens might not be statistically different. Similar to their Log K_{ow} values, their 95% confidence intervals overlapped. With the 95% confidence intervals, $1/n$ values for E1, E2, EE2 were 0.699 ± 0.087 , 0.584 ± 0.078 and 0.449 ± 0.120 .

The adsorptive energy also appeared to be stronger for the higher EE2 concentration as indicated by the lower $1/n$ value (0.259). However, the 95% confidence interval of $1/n$ value (0.116 – 0.401) obtained for the higher initial

concentration of EE2 overlaps with the 95% confidence interval (0.329 – 0.570) calculated for the lower initial concentration of the same compound, suggesting that the adsorptive energy might not be statistically different for the two different initial concentrations of EE2.

Some effect of the difference in initial concentration was seen in the Langmuir and Freundlich parameter for the adsorption of EE2 onto CBV-780. Adsorption equilibrium with the higher initial concentration (6.24 mg/L) showed larger q_{max} value (145 mg/g) compared to q_{max} (102 mg/g) for the lower initial concentration (1.63 mg/L). Erdem-Şenatalar *et al.* (2004) found that DAY adsorbed methyl tertiary butyl ether (MBTE), with the estimated dimension of $5.75 \text{ \AA} \times 5.93 \text{ \AA} \times 7.2 \text{ \AA}$, more effectively at higher initial concentrations than at lower initial concentrations. Giaya *et al.* (2000) explained, in certain condition, adsorption capacity may more accurately depend on “who got there first”. If a hydrophobic organic compound enters the hydrophobic pores of an adsorbent, it is expected to enhance the exclusion of water molecules. In the case with the higher EE2 concentration, more EE2 molecules are likely to come in contact with hydrophobic zeolite than at the lower concentration of EE2. Thus, increased EE2 molecular contact with the zeolite might have dominated the transient process resulting in the higher EE2 mass adsorption onto zeolite CBV-780.

Tsai *et al.* (2006) found that the amount of adsorbate taken up by zeolite is proportional to its mass and initial concentration. In their study with another EDC, bisphenol A (BPA), they found q_e (mg/g) increased as the initial concentration of the contaminant increased. It was primarily due to the increase in the concentration

gradient. Delle Site (2001) stated that in the case of hydrophobic molecules the relatively weak bonding forces associated with physical sorption are often amplified by substantial thermodynamic gradients for repulsion from the solution in which they are dissolved.

However, the accumulation of adsorbate mass on an adsorbent would inversely affect the adsorption frequency and hence the adsorption rate constant, as the adsorption sites would get scarce with increasing adsorption. Tsai *et al.* (2006) noticed that the values of half of the adsorption time, $t_{0.5}$, for BPA increased from 0.05 to 3.93 min as the initial BPA concentration increased from 10 to 90 mg/dm³ (= 90 mg/L).

4.2.4. Adsorption of the estrogens on the zeolite CBV-901

As in the case of CBV-780, adsorption isotherms were developed for CBV-901. Figure 4.9 shows the nonlinear adsorption isotherms for E1, E2 and EE2 on CBV-901.

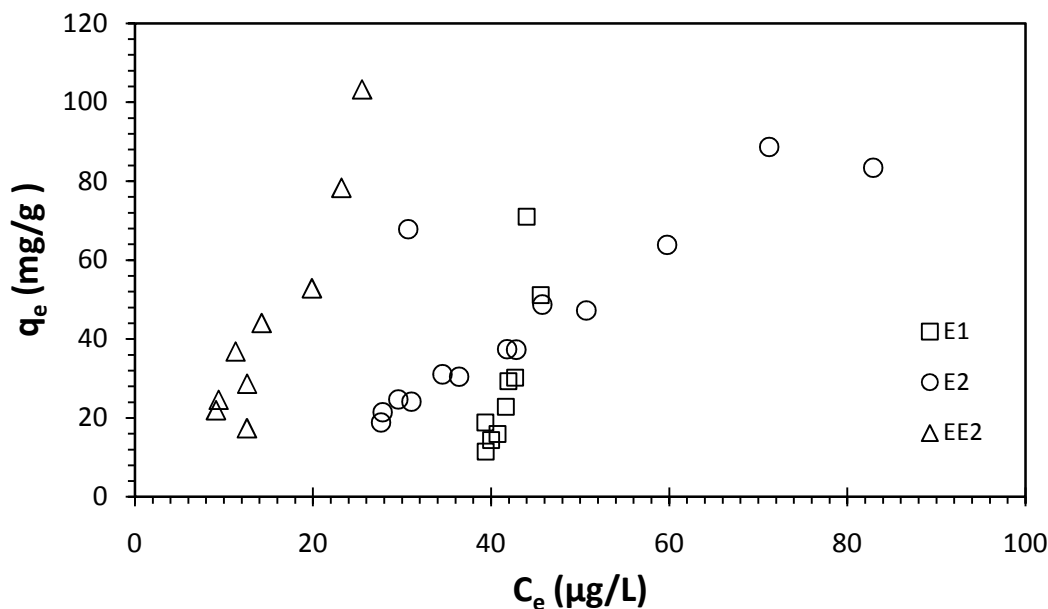


Figure 4.9 Adsorption isotherms of E1, E2 and EE2 on CBV-901

Wen *et al.* (2009) observed bi-phase E1 adsorption on DAY. To examine if this affect was observed for CBV-901, we included a second adsorption study utilizing low concentrations (≤ 15 mg/L) of zeolite. The results obtained are displayed and compared to data from Wen *et al.* (2009) in Figure 4.10. The q_e values obtained in this study lie above the Wen *et al.* (2009) data, displaying higher adsorption capacity of zeolite Y.

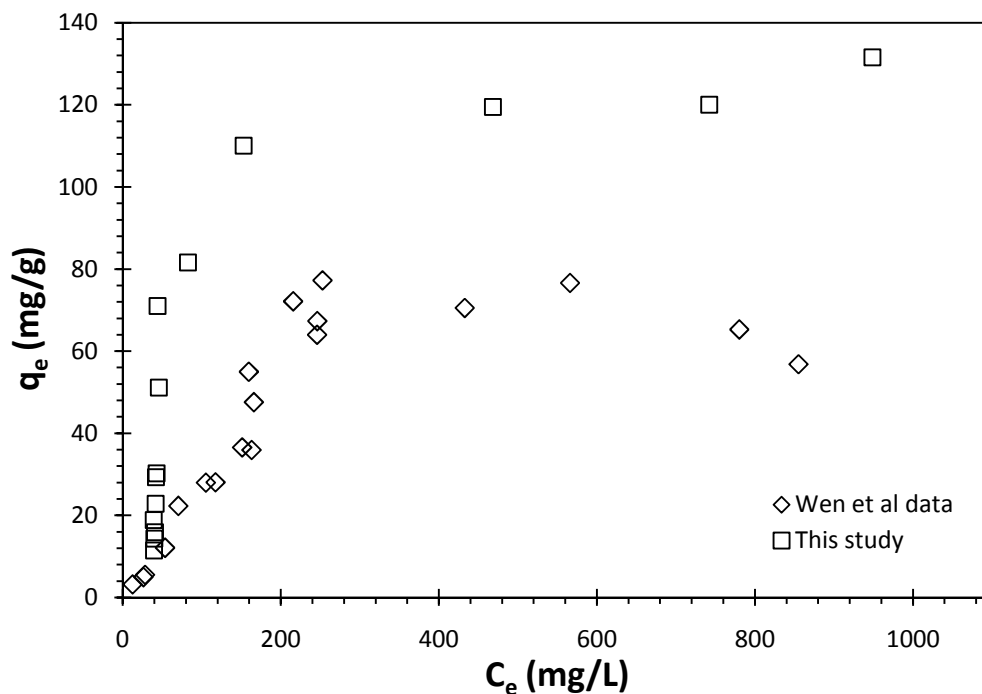


Figure 4.10 Comparison of adsorption equilibrium data from Wen *et al.* (2009) with values obtained in this study

Figures 4.11 and 4.12 illustrate the linearized Freundlich and Langmuir isotherms, respectively. The data sets shown in Figure 4.9 were used in developing the linearized models. Considering the assumptions of the Freundlich model where q_e increases with C_e , only E1 Phase-1 data shown in Figure 4.9 was used for generating the Freundlich isotherm for this EDC. As demonstrated by the high correlation factors, R^2 values, both the models appeared to be good fits for the adsorption of all three estrogens: E1, E2 and EE2 on CBV-901.

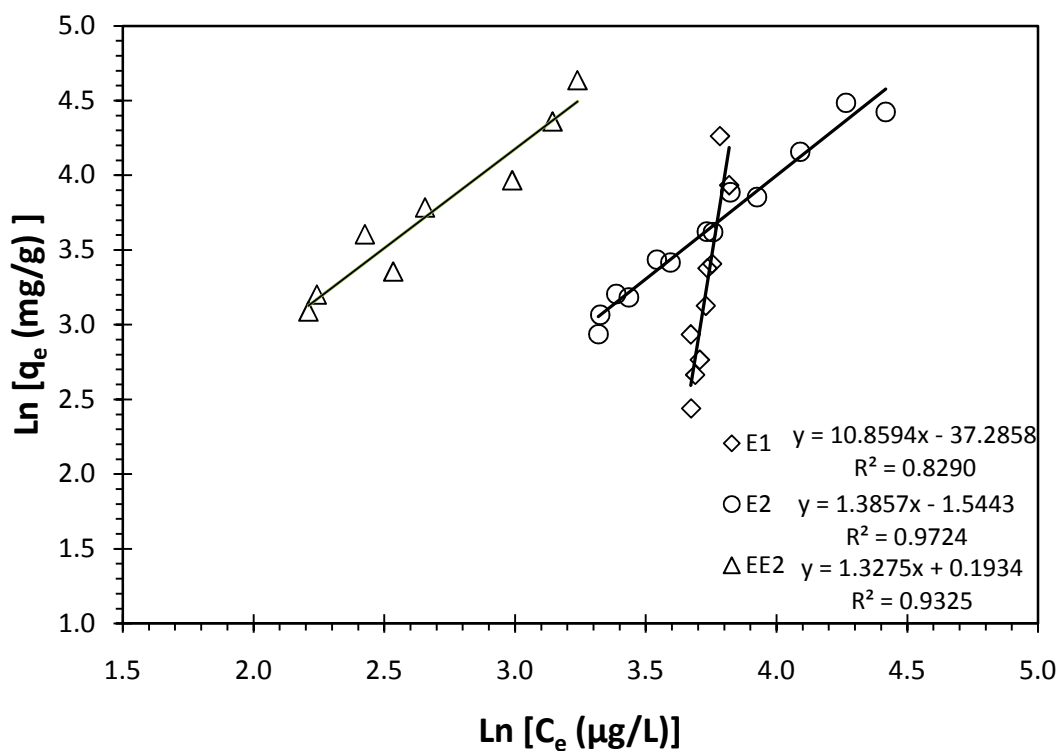


Figure 4.11 The linearized Freundlich isotherms of E1, E2 and EE2 on CBV-901

Figure 4.11 shows an almost vertical plot for E1, with most of the data points at the equilibrium concentration, C_e of 40 $\mu\text{g/L}$. It is possible that the concentrations were in ng/L range but could not be quantified with the analytical method available. Thus, similar C_e values appear to have the same q_e values, which disagree with the assumptions in the Freundlich isotherm that says q_e increases as C_e increases. Consequently, the Freundlich parameters $1/n$ and K_F could not be estimated appropriately.

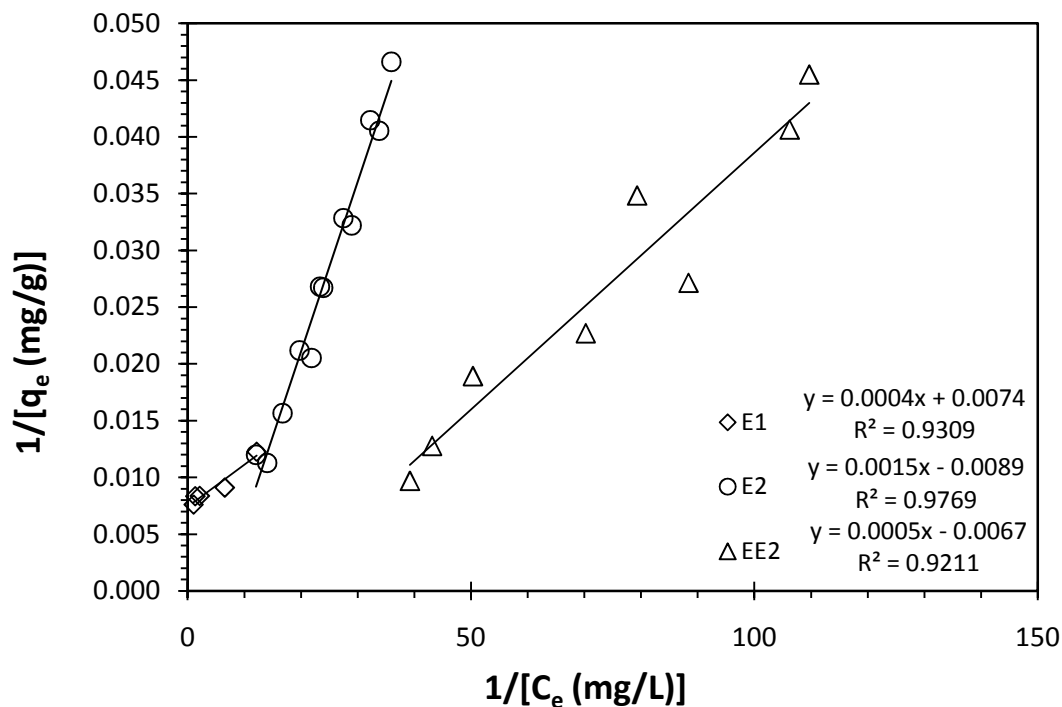


Figure 4.12 The linearized Langmuir isotherms of E1, E2 and EE2 on CBV-901

The Freundlich and Langmuir parameters obtained from the linearized models in Figures 4.11 and 4.12 are shown in Table 4.2. Like in the case of CBV-780, CBV-901 showed revealed the lowest adsorption capacity, q_{max} (112 mg/g) for E2, but the order of q_{max} values for E1 and EE2 were reversed. EE2 had the higher q_{max} value (149 mg/g) than E1 (135 mg/g). The Freundlich constant, K_F , which is also indicative of the adsorption capacity followed the trend of q_{max} values for E2 and EE2.

Unlike in the case of CBV-780, q_{max} values for the higher and the lower concentrations of EE2 appeared to be similar (Table 4.2). This might be suggesting that the difference in the initial concentration may affect the rate of removal, as explained in the earlier section, rather than the ultimate adsorption capacity of an adsorbent for an adsorbate.

Table 4.2 Summary of adsorption isotherm parameters for CBV -901

Zeolite	EDC	Langmuir Parameters		Freundlich Parameters	
		q_{max} (mg/g)	b (L/g)	$1/n$	K_F [(mg/g)•(L/μg) ^{1/n}]
CBV-901	E1 (1.33 mg/L)	135	18.5	10.9	0.00
	E2 (1.40 mg/L)	112	5.93	1.39	0.21
	EE2 (1.57 mg/L)	149	13.4	1.33	1.21
	EE2 (6.0 mg/L)	141	35.5	0.126	57.0

As indicated by $1/n$ values (Table 4.2), the higher adsorption energy was observed for the low-concentration EE2, followed by and E2 and E1. In this case also 95% confidence intervals of $1/n$ values calculated for E2 and EE2 overlapped suggesting no distinct trend in their adsorptive energies.. With the 95% confidence intervals, $1/n$ values for E1, E2, EE2 were 10.9 ± 4.41 , 1.39 ± 0.155 and 1.33 ± 0.357 .

Again, the demonstrated adsorptive energy trend does not correlate with the recommended single Log K_{ow} values for each compound, but agreed more with the range of Log K_{ow} values provided by LOGKOW© (accessed April 2010).

4.2.5. CBV-780 versus CBV-901

When adsorption capacities of CBV-780 and -901 were compared, 20 mg/L of CBV-901 reduced over 95% of E1, E2 and EE2. Thus, it appeared to be a better adsorbent than CBV-780 which removed similar amounts of the estrogens at 60 mg/L (Figure 4.1). When adsorption isotherms were generated for both the zeolites, CBV-901 showed higher q_{max} values (Table 4.2) and hence the higher adsorption capacities for the estrogens than CBV-780 (Table 4.1).

According to the specifications provided by the manufacturer (Appendix A) CBV-780 and -901 had similar Si/Al ratio but their specific surface areas were different. CBV-780 had a surface area of 861 m²/g and CBV-901 had a surface area of 743 m²/g. Despite having the larger surface area, CBV-780 did not perform better than CBV-901.

Normally, a larger surface area has been considered favorable for adsorption; however, it has not been the dominant characteristic dictating adsorption. Wen *et al.* (2009) compared activated carbon and DAY for removal of E1. Activated carbon and DAY had specific surface areas of 1014 and 692 m²/g, respectively, but activated carbon was able to remove only 69% of E1 compared to 99% removed by DAY. Activated carbon had the largest pore dimension, on average of 7.8 Å and the total specific pore volume of 0.51 m³/g. DAY had the largest pore dimension, on average of 7.4 Å and the total specific pore volume of 0.38 m³/g (Wen *et al.*, 2009).

Khalid *et al.* (2004) found that zeolite performed better as an adsorbent than activated carbon at low concentrations of phenol. They attributed the inferior performance of activated carbon to its wide range of pore structures which allowed phenol molecules to diffuse rapidly inside the activated carbon pores and also desorb easily during the process. Similar phenomenon may be occurring in the case of CBV-780. Given its larger surface area (861 m²/g), it might have a bigger pore structure compared to CBV-901 with the smaller surface area (743 m²/g). This is similar to the case in Wen *et al.* (2009) study where activated carbon with the larger surface area (1014 m²/g) had the larger pore volume of 0.51 m³/g compared to zeolite with the lower surface area (692 m²/g) and the smaller pore volume of 0.38 m³/g. Thus, CBV-

901 might be more size selective than CBV-780 for the adsorption of small EDC molecules examined in this study.

Adsorbents are known to have a varying adsorption capacity dictated by a structure effect, due to which faujasites in general were found to have a far higher adsorption capacity than silicalites (Reungoat *et al.*, 2007). The zeolites used in this study were zeolite Y which is a subset of faujasites. Khalid *et al.* (2004) found that for zeolites with Si/Al ratio between 16 – 100 pore structures seem to be a significant parameter for adsorption.

Thus, more than the respective surface area, the pore structures might be dictating the adsorption capacities of CBV-780 and -901. Also, they might have different ratios of internal pore surface area to the external surface area. It is important because Wen *et al.* (2009) reported that only about 16% of the DAY pore volume was filled at saturation. Based on this low level of pore filling and the plateau in the isotherm observed, they hypothesized that E1 existing as pure crystal or precipitated solid or quasi-solid could have blocked the pore throats, subsequently inhibiting higher loadings into the internal pore volumes. If CBV-901 particles were smaller and had a larger external surface area per unit mass than CBV-780, occurrence of such pore blockage phenomenon would favor adsorbate mass loading on CBV-901.

Another factor which might be enhancing the adsorption capacity of CBV-901 may be the slightly higher hydrophobicity as indicated by Si/Al ratio of 41.3 compared to 40.5 of CBV-780. Also, communications with the manufacturer indicated that CBV-901 is modified material that, although having the same chemical analysis as CBV-780, is much more hydrophobic resulting in improved adsorption

properties. A possible modification could be further dealumination of unit cells resulting in the higher Si/Al ratio than reported.

Giaya *et al.* (2000) suggested, other parameters such as wetting angle might be affecting the sorption capacity, when they found varying adsorption capacities for three adsorbents (DAY, Silicate-1 and Centaur© activated carbon) with identical values for the hydrophobicity.

4.3. Regenerative Ability of Zeolites

During the regeneration processes 30 minutes was selected as the MP UV irradiation time. Within this time, all three compounds showed complete degradation in the aqueous phase, in the absence of zeolites when irradiated with the MP UV lamp as shown in Figures C-1 through C-3 (Appendix C).

Zeolite CBV-780 was selected for the regeneration experiments. Figure 4.13 illustrates the remaining E1 concentration in the solution after equilibrating for an hour on an orbital shaker. “0” regeneration cycle on the x-axis indicates when the zeolites were first exposed to E1 solution. Each regeneration cycle-number is associated with the number of times the same mass of zeolites was regenerated. The bars above Regeneration cycle-1 show the reduced E1 concentration obtained after the zeolites regenerated once were mixed into the fresh E1 stock solution. The concentration of E1 stock solution used for these experiments was 1.03 mg/L.

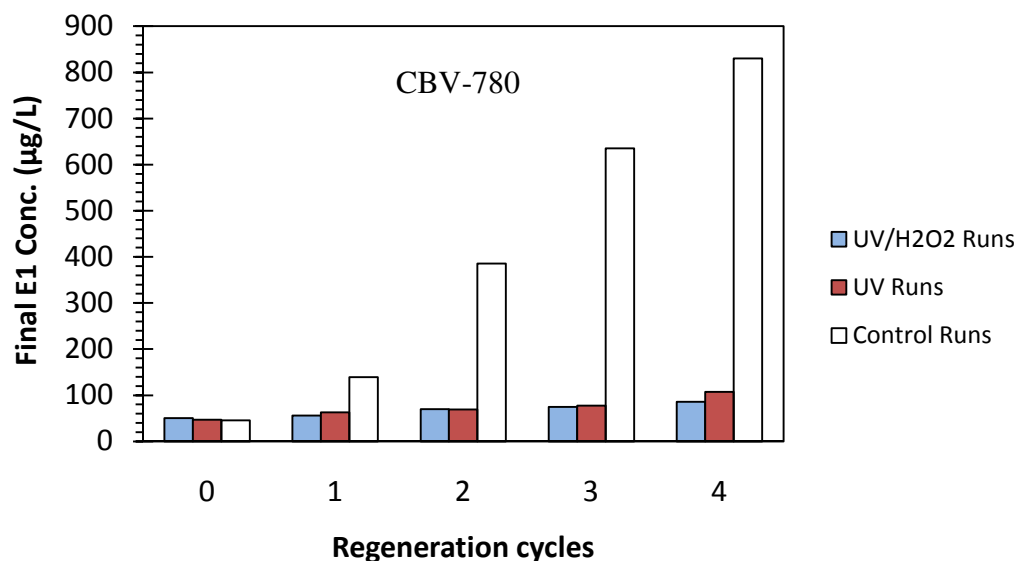


Figure 4.13 Remaining E1 concentration during UV photolysis and UV AOP as compared to untreated zeolites case

From Figure 4.13, it can be observed that the virgin zeolites were able to reduce 1.03 mg/L of E1 to a concentration less than 50 µg/L. After multiple adsorption / regeneration cycles, the equilibrium concentration of E1 remained low for UV/H₂O₂ and UV treated zeolites, but increased markedly for the control case, where zeolites did not receive any UV regeneration treatment. Even after the 4th regeneration event, equilibrium concentration of E1 for UV/H₂O₂ and UV regenerated cases remained below 100 µg/L; while the aqueous E1 concentration for the control case exceeded 800 µg/L. As a result, the regenerated zeolites adsorbed nearly twice as much E1 mass as the untreated zeolites (Figure 4.14).

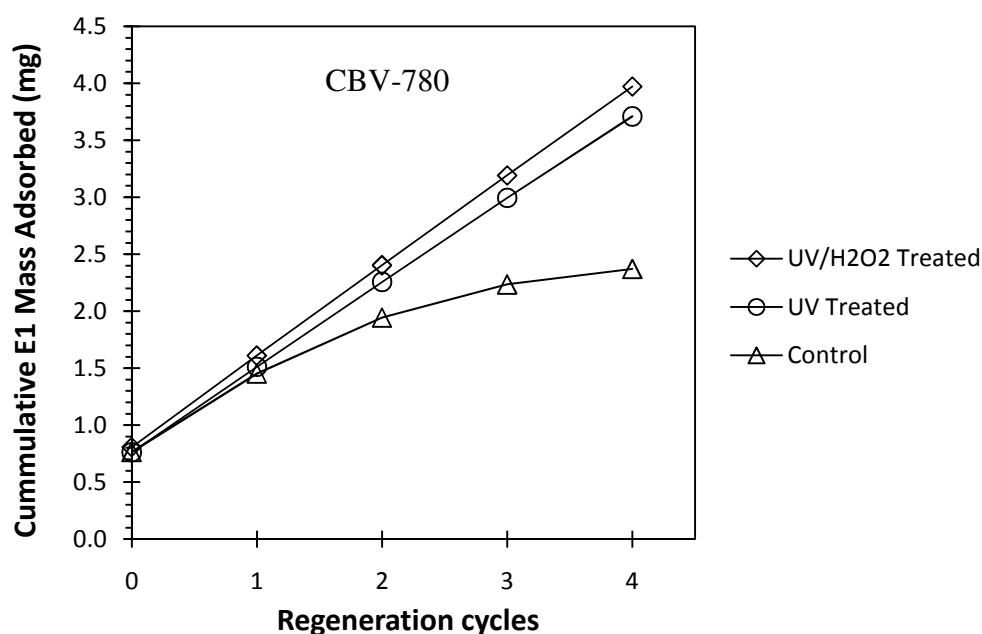


Figure 4.14 Comparison of cumulative E1 mass adsorbed by zeolites treated with UV and UV AOP; and untreated zeolites

The total mass of E1 adsorbed by UV/H₂O₂ and UV regenerated zeolites were 4.0 and 3.7 mg, respectively, after four cycles. The untreated zeolite adsorbed 2.4 mg of E1, in total. As presented by both the Figures 4.13 and 4.14, adding 10 mg/L of H₂O₂ did not significantly enhance the removal process. By the end of the 4th regeneration cycle, UV/H₂O₂ treated zeolites removed only 8% more than the UV treated zeolites.

Figure 4.15 shows the reduction in E2 concentration over 4 regeneration cycles. As in the case of E1, initially (Regeneration cycle-0) all three batches of zeolites removed E2 equally well from the aqueous solution. With the successive regeneration cycles, the disparity between the equilibrium concentrations increased.

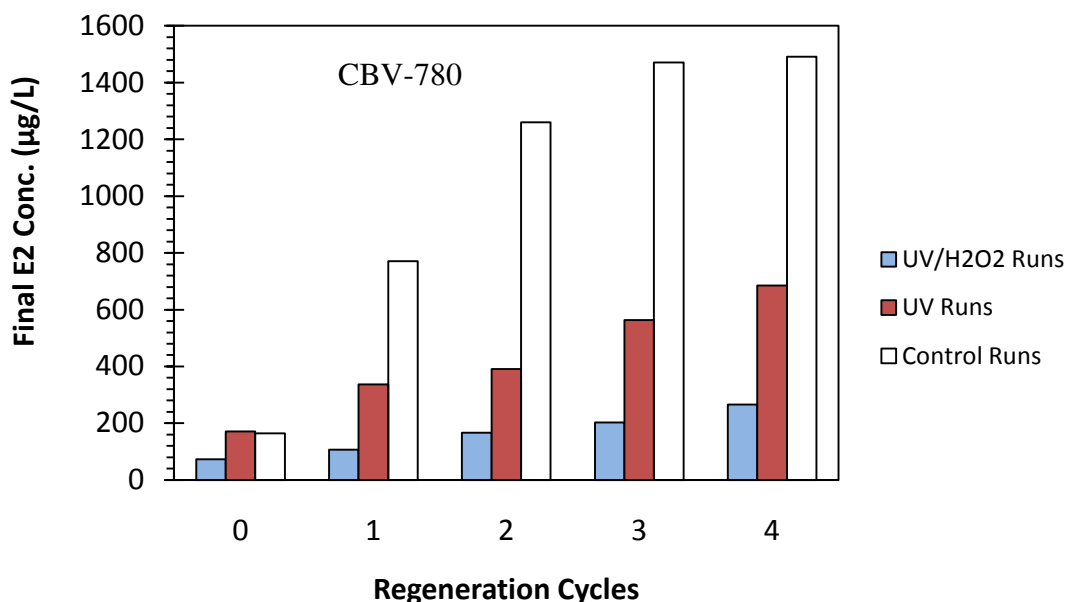


Figure 4.15 Remaining E2 concentration during UV photolysis and UV AOP as compared to untreated zeolites case

The remaining concentrations of E2 after 4 regeneration cycles were 270, 690 and 1490 µg/L for the UV/H₂O₂, UV and control treatments, respectively. The untreated zeolites (control) were saturated even before the onset of the 4th regeneration cycle (Figure 4.15) because the final concentration achieved after the 3rd regeneration cycle was close to the initial concentration of the stock solution used. Compared to the results obtained for E1, UV/H₂O₂ and UV treated zeolites showed larger difference in reduction of E2 concentration. This was because the solution used for UV/H₂O₂ treatment had 1.40 mg/L, and the one used for UV treatment had 1.50 mg/L, of E2. Although both the treatments removed similar amount of E2 mass as demonstrated by Figure 4.16, the remaining concentration in UV treatment appeared to be higher because there was more E2 to begin with. Thus, in terms of removal capacity

UV/H₂O₂ and UV treatment were comparable and the discrepancy in the remaining E2 aqueous concentration was an artifact of slightly different initial concentrations.

Figure 4.16 shows the cumulative E2 mass adsorbed by different batches of zeolites. The UV/H₂O₂ and UV treated zeolites removed 4.9 and 5.0 mg, respectively. The untreated batch of zeolites removed 2.7 mg. Thus, the regenerated zeolites removed almost twice as much mass of E2 than the untreated zeolites, and there was no significant difference between UV/H₂O₂ and UV treated zeolites in regards to the adsorption capacity at the end of the 4th regeneration cycle.

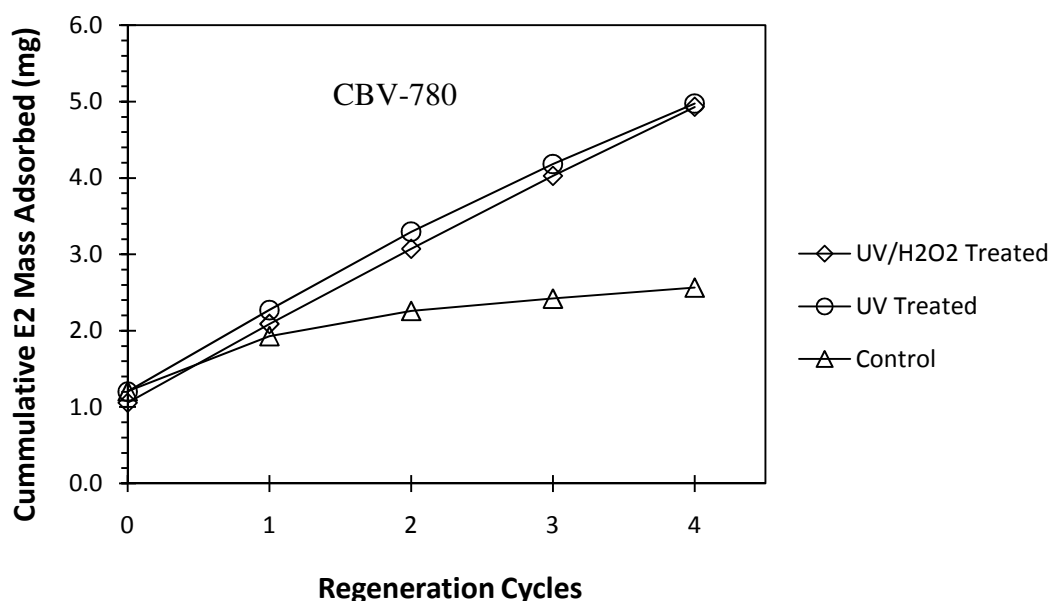


Figure 4.16 Comparison of cumulative E2 mass adsorbed by zeolites treated with UV and UV AOP; and untreated zeolites

Figure 4.17 shows the remaining concentrations of EE2 at each adsorption equilibrium step during the regeneration process. Like in the prior cases, the UV/H₂O₂ and UV treated zeolites consistently removed high amounts of EE2 in the

subsequent regeneration cycles, while adsorption by the untreated zeolites declined over the regeneration cycles. As a result, the equilibrium concentrations achieved by the UV/H₂O₂ and UV treatment after the 4th regeneration event were 420 and 610 µg/L, respectively. Whereas, the untreated zeolites left 1550 µg/L of E2 unadsorbed in the final equilibrium solution. The initial concentration of EE2 solution was 1640 µg/L for the UV/H₂O₂ treatment and 1630 µg/L for the UV and control cases.

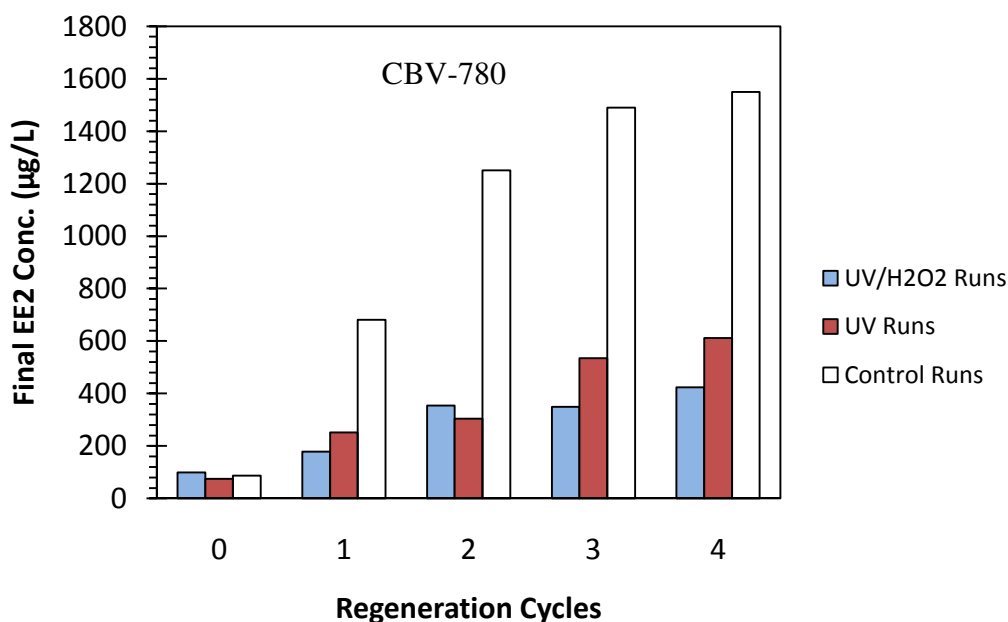


Figure 4.17 Remaining EE2 concentration during UV photolysis and UV AOP as compared to untreated zeolites case

Figure 4.18 shows the cumulative EE2 mass removed by zeolites during the regeneration experiment. The UV/H₂O₂, UV and control setups removed 5.4, 5.1 and 2.5 mg of EE2, respectively. Here, the UV/H₂O₂ treatment removed about 6% more EE2 mass than the UV photolysis, and both the UV/H₂O₂ and UV treatment removed more than double the mass removed by the untreated zeolites.

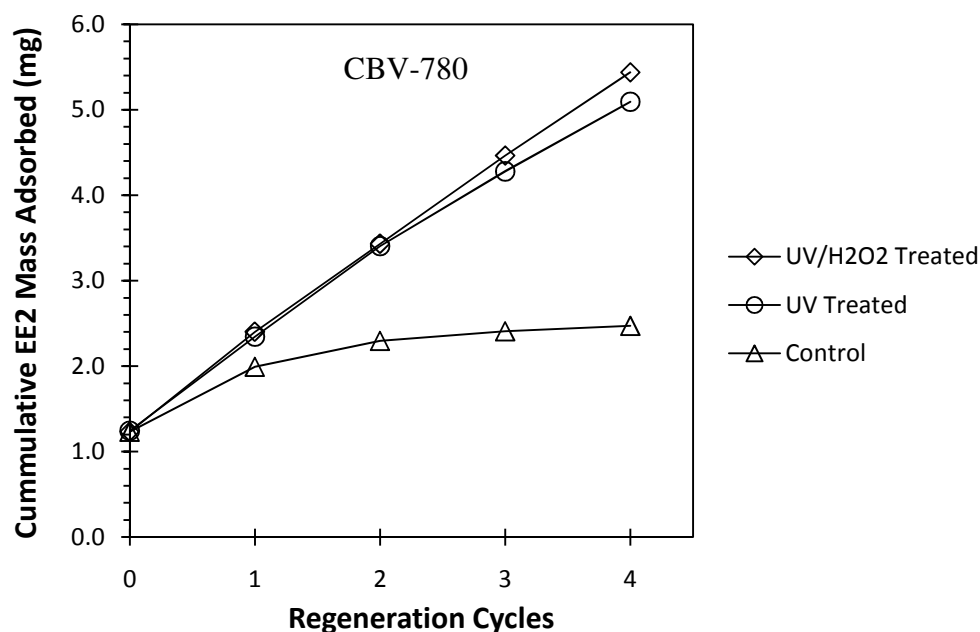


Figure 4.18 Comparison of cumulative EE2 mass adsorbed by zeolites treated with UV and UV AOP; and untreated zeolites

4.4. Dose Response in Regeneration

Studies have shown that addition of a strong oxidant like H_2O_2 to UV processes enhances the degradation of trace contaminants such as E2 and EE2 (Rosenfeldt *et al.*, 2004, 2007). Rosenfeldt and Linden (2004) showed that UV/ H_2O_2 degraded EDCs (BPA, E2 and EE2) more effectively than UV photolysis treatment. The UV/ H_2O_2 treatment removed approximately 70% more EDCs than UV photolysis. The lack of such difference in EDC removal in this study may be attributed to issues associated with the transport of hydroxyl radical to the target contaminant.

In the study conducted by Rosenfeldt and Linden (2004) EDCs were present in aqueous solution. Hence, hydroxyl radicals, formed after the absorption of UV radiation by H_2O_2 molecules, readily came in contact with dissolved EDC, resulting

in their oxidation. But, in this study EDCs were adsorbed onto zeolites, which made the EDCs less available to the aqueous hydroxyl radicals. Hydroxyl radicals formed in solution must transport a certain distance to come in contact with the EDCs attached to zeolites. As the hydroxyl radicals are highly reactive particles they are mostly consumed soon after their formation. We postulate that only the hydroxyl radicals formed due to the breakdown of H_2O_2 molecules in the immediate vicinity of zeolite particles can oxidize the EDCs attached to the particles. Therefore, UV AOP would not be as effective when EDCs are attached to zeolites versus a homogeneous aqueous solution.

Another possible explanation for the minimal difference in the performance of the UV/ H_2O_2 and UV treated zeolites could be related to the excessive UV dose provided (30 minutes of UV), which efficiently degrade the compounds even in the absence of H_2O_2 , given the initial concentration of the contaminant used. To test this hypothesis UV treatment was carried out at lower UV doses. The result of this test is illustrated in Figure 4.19. The figure shows no significant difference in the performance of zeolites treated with 30, 15 or 5 minutes of UV in the first regeneration cycle. However, relatively larger difference in E2 reduction was noticed in adsorption equilibrium in the 2nd regeneration cycle. The UV irradiation times and the associated doses are illustrated in Table 4.3.

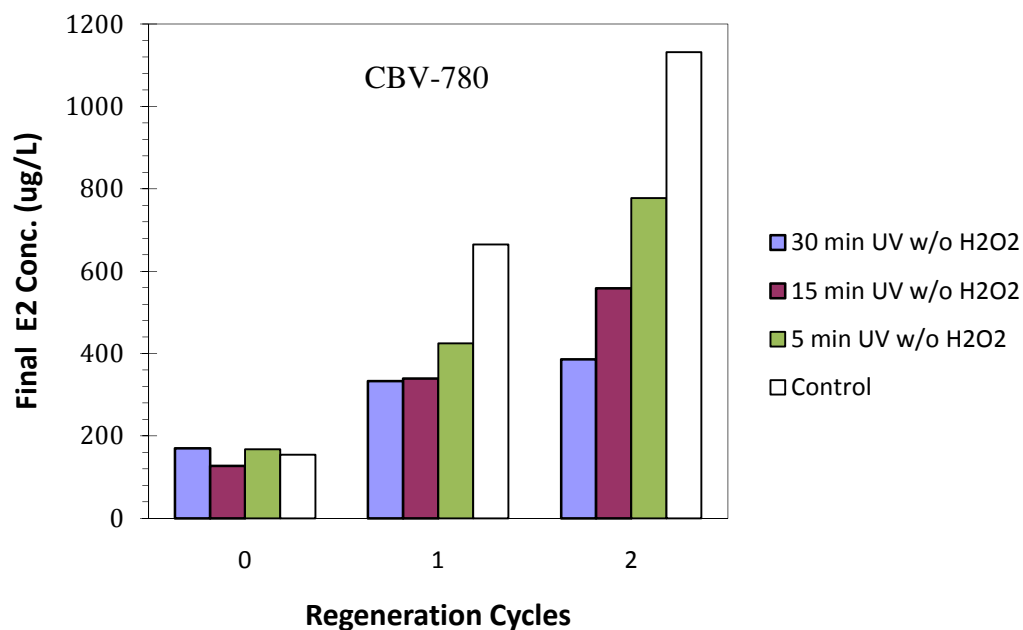


Figure 4.19 Comparison of E2 degradation between different UV irradiation times

Table 4.3 UV irradiation times and the corresponding UV dose

UV Irradiation Time (min)	Approximate UV Dose (mW/cm ²)
30	8000
15	4000
5	1300
Control	0

The initial concentration of E2 used for the 30-minute UV experiment was 1.60 mg/L and for 15- and 5-minute UV experiments, 1.50 mg/L of E2 aqueous solution was used. After the 2nd regeneration cycle, the total E2 mass adsorbed by the zeolites regenerated with 30 minutes of UV irradiation was 3.2 mg (Figure 4.20). The control

experiment conducted concurrently removed only 2.2 mg of E2. The total E2 mass adsorbed by zeolites irradiated with 15 and 5 minutes of UV were 2.8 and 2.4 mg, respectively (Figure 4.20). The control experiments for both, 15- and 5-minute UV experiments removed 2.0 mg of E2.

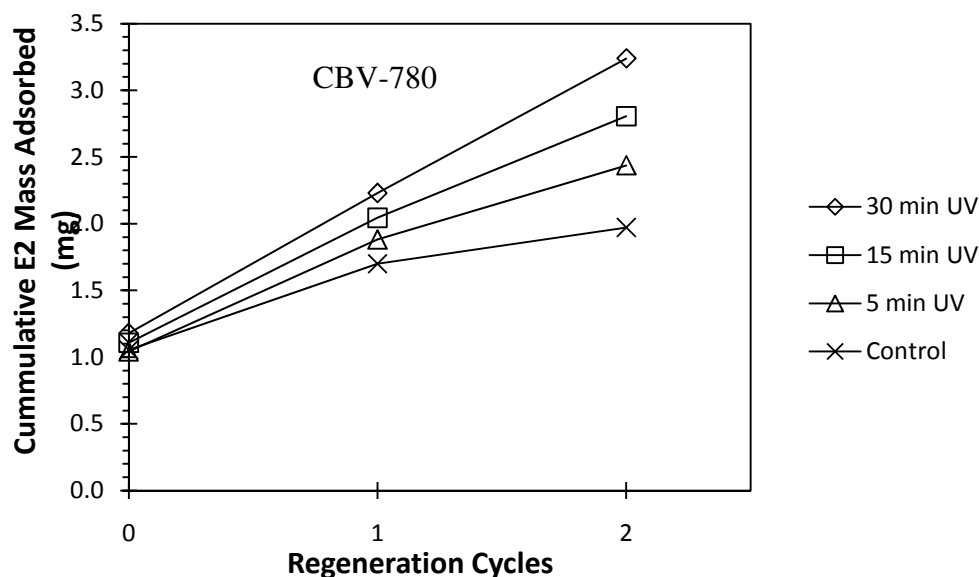


Figure 4.20 Comparison of cumulative E2 mass adsorbed by zeolites treated with 30 to 5 minutes of UV

Zeolites irradiated with 30 minutes of UV adsorbed approximately 13% and 25% more E2 mass than the ones irradiated with 15 and 5 minutes of UV, respectively, after two regeneration cycles. The zeolites irradiated with 15 minutes of UV adsorbed about 14% more E2 mass than those irradiated with 5 minutes of UV. Since there was larger difference in the mass adsorbed by zeolites irradiated with 30 and 5 minutes of UV, further investigation was carried out to see if addition of H_2O_2 would enhance the adsorption capacity of zeolites irradiated with 5 minutes of UV. The result of this test is illustrated in Figure 4.21.

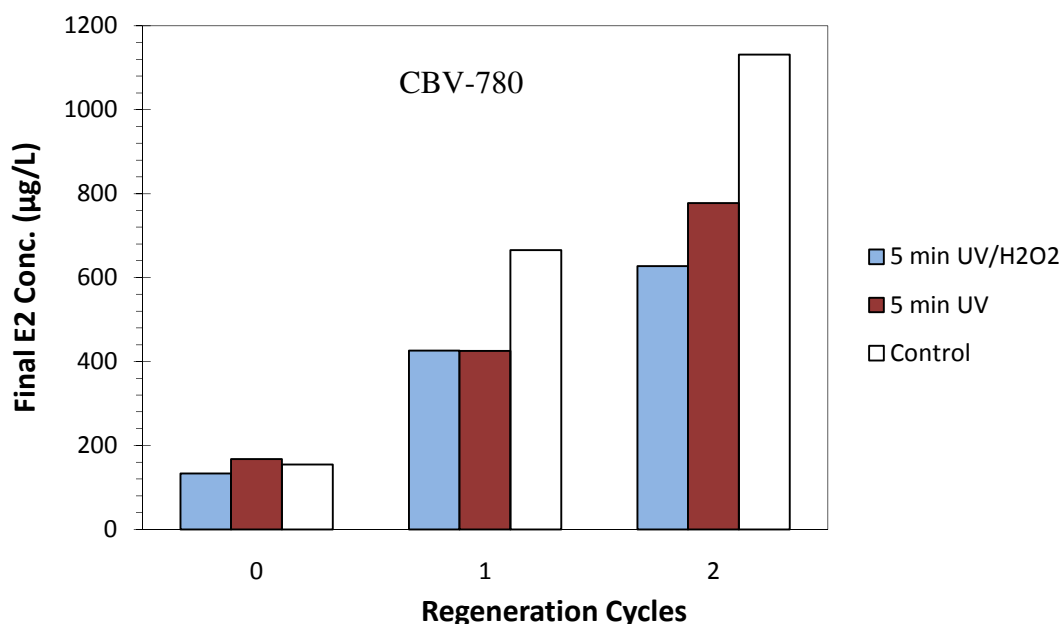


Figure 4.21 Remaining E2 concentration in UV/H₂O₂ and UV treatment compared to control experiment

In 5-minute UV irradiation experiment, by the end of 2nd regeneration cycle, the UV/H₂O₂ treatment removed 2.7 mg of E2 from aqueous solution while, the UV treatment removed 2.5 mg of E2 (Figure 4.22). The initial concentration of E2 stock used was 1.50 mg/L for both the treatments. Thus, UV/H₂O₂ removed about 7% more than the UV only treatment. The trends for 5-minute UV exposure are similar to those trend observed for the 30-minute exposures.

Thus, the comparison of 30- and 5-minute UV experiments revealed that H₂O₂ does not enhance the estrogen degradation even if lower UV doses are used. This supports the argument that the lack of enhanced degradation via the UV/H₂O₂ treatment may have been due to the high reactivity of hydroxyl radicals formed which got consumed before they could come in contact with zeolite-adsorbed-EDCs. More

so, because the zeolite concentration was the same in both the 30- and 5-minute UV experiments, and the initial concentrations of E2 were also comparable.

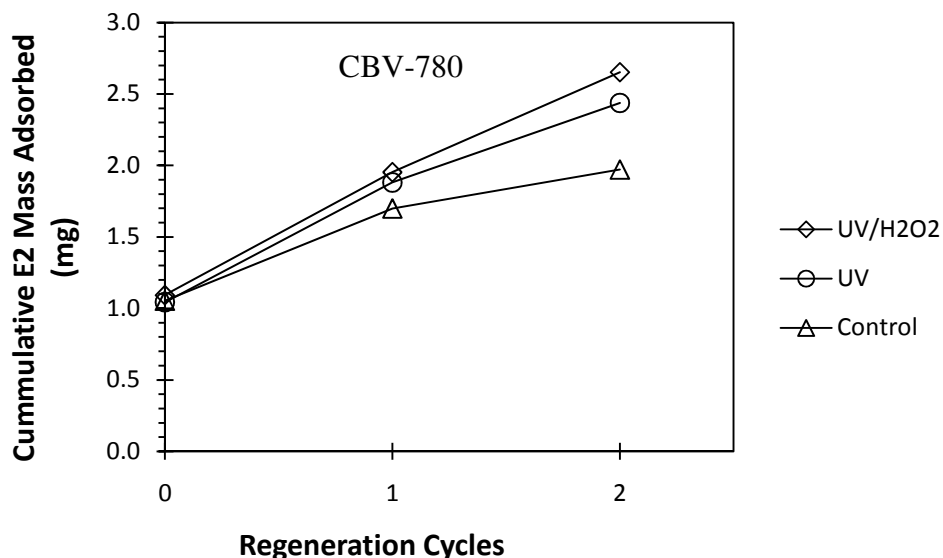


Figure 4.22 Comparison of cumulative E2 mass adsorbed by zeolites treated with UV and UV AOP; and untreated zeolites

4.5. Adsorption in Natural Waters

After successful quantification of the adsorption capacity and the regenerative ability of zeolites in deionized water (DI), investigation was done to quantify similar parameters and test the efficacy of regeneration methodology in natural waters. From a water treatment plant in Northampton, MA, two sets of water samples were collected; raw water entering the treatment train, and post-filter water which had already undergone coagulation, flocculation and filtration. The results of water quality analysis of the two samples collected are shown below in Table 4.4. The detection limits of the equipments used for the analysis are shown in Appendix E.

Water samples were filtered through 0.45 μm filter for the analysis of water quality parameters, and performance of adsorption experiments.

Table 4.4 Water quality parameters (all in mg/L) of natural water samples

Sample ID	Na	K	Mg	Ca	Fe	Chloride	Sulfate	Nitrate	Phosphate	Dissolved Inorganic Carbon	Dissolved Organic Carbon	Total Nitrogen
Post Filter	3.67	0.63	0.74	5.32	0.01	4.63	8.32	ND	ND	3.51	1.09	0.07
Raw	1.81	0.60	0.72	5.17	0.05	1.96	3.95	ND	ND	3.78	2.08	0.14

Similar to the methodology with deionized water, adsorption equilibrium experiments were performed to test the adsorption capacity of zeolites in natural water. Figure 4.23 compares degradation of E2 with increasing zeolite concentration in natural waters and DI. The initial concentrations of E2 were same, about 1.6 mg/L, in all three cases.

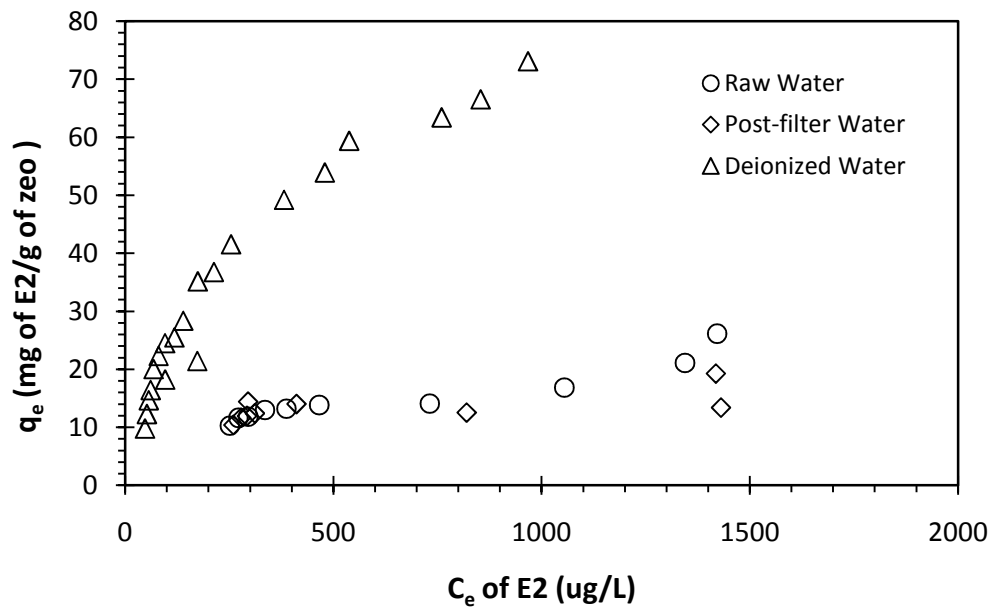


Figure 4.23 Adsorption isotherms of E2 on CBV-780 in DI and natural waters

As shown in Figure 4.23, in natural waters, less E2 was adsorbed by the same amount of zeolites than in DI water. This was possibly due to the presence of organic and inorganic carbon, and other substances including iron, magnesium, calcium salts and other precipitates in natural waters, which could be interfering with E2 adsorption via deposition on the adsorbent (Snoeyink and Summers 1999). Thus, to test, if in fact these substances were adsorbing onto the zeolites, an equilibrium experiment was conducted with only zeolite CBV-780 in natural water. The solutions were left overnight on an orbital shaker at 275 RPM. Water quality analysis of natural water was performed before and after adsorption. The concentrations of the zeolite used and the results obtained are shown in Table 4.5.

The water quality analysis showed reduction in inorganic carbon, calcium, magnesium and sulfate as the applied dose of CBV-780 increased. This indicates potential formation of precipitates of these compounds which may be depositing on the surface of zeolites, blocking pore throats and inhibiting adsorption of E2.

However, no reduction was observed in the organic carbon contents of the water prior to and after adsorption equilibrium. Thus, organic carbon may not be inhibiting the adsorption of E2 onto zeolite in this case. Although hydrophobic, molecules of organic carbon compounds are generally large in size, and hence are excluded from 7.4 Å (Wen *et al.*, 2009; Reungoat *et al.*, 2007) pore diameter of DAY zeolites, like the ones used in this study. Whereas, E2 ($C_{18}H_{24}O_2$), similar in size as E1 ($C_{18}H_{22}O_2$) which is 4Å × 11Å (Wen *et al.*, 2009) could easily diffuse into zeolites pores and be removed from the aqueous solution.

Table 4.5 Water quality analysis of post-filter and raw water before and after adsorption equilibrium experiments with zeolite CBV-780

Water	CBV-780 Conc. (mg/L)	Na (mg/L)	K (mg/L)	Mg (mg/L)	Ca (mg/L)	Fe (mg/L)	Chloride (mg/L)	Sulfate (mg/L)	Nitrate (mg/L)	Phosphate (mg/L)	TOC (mg/L)	Inorganic Carbon (mg/L)	TN (mg/L)
Post-filter	0	3.69	0.54	0.76	5.70	BDL	4.58	8.23	BDL	ND	0.92	3.14	0.08
	10	3.80	0.58	0.77	5.70	BDL	4.60	8.20	BDL	ND	0.98	3.04	0.05
	100	3.71	0.53	0.73	5.42	BDL	4.58	8.17	ND	ND	0.98	2.91	0.05
	995	3.69	0.53	0.57	3.76	ND	4.60	8.14	0.05	ND	1.32	2.07	0.08
Raw	0	1.98	0.55	0.76	5.60	BDL	1.89	4.09	0.17	ND	1.67	3.92	0.11
	10	1.94	0.53	0.75	5.55	BDL	1.91	3.88	0.18	ND	1.67	3.80	0.11
	101	1.97	0.54	0.74	5.42	BDL	1.99	3.98	0.20	ND	1.65	3.58	0.11
	1002	1.96	0.55	0.54	3.57	BDL	1.91	3.97	0.21	ND	2.13	2.54	0.13

The linearized Freundlich and Langmuir adsorption isotherms developed for DI and natural waters are shown in Figures 4.24 and 4.25, respectively. Freundlich model did not work well for all three conditions in relation to the correlation coefficient R^2 . The post-filter water showed the poorest correlation in the data, followed by the raw water results. The Freundlich equation might not have worked for the post-filter water due to the saturation of adsorbent, which is also indicated by the plateauing of the post-filter curve in Figure 4.23. In accordance to equation 4.1, q_e increases as C_e increases, only until the adsorbent approaches saturation. Once the saturation is attained, q_e remains constant and is independent of further increase in C_e , consequently disagreeing with assumptions associated with the Freundlich equation (Snoeyink and Summers 1999).

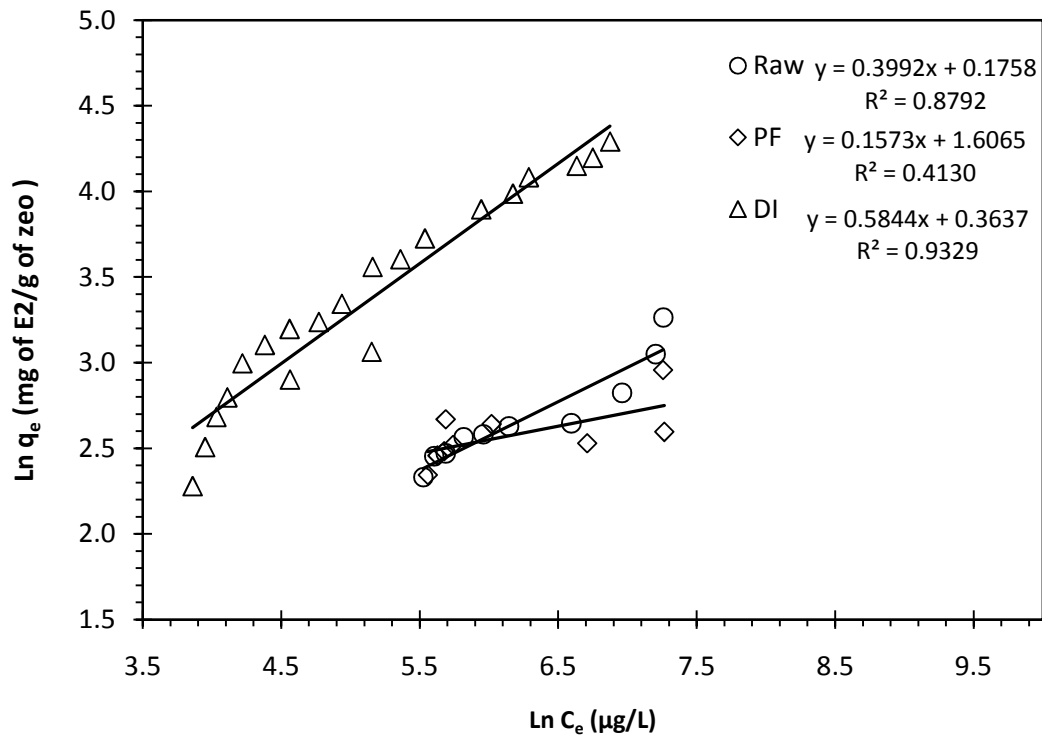


Figure 4.24 The linearized Freundlich isotherm of adsorption of E2 in natural water on CBV-780

Like the Freundlich isotherm, the Langmuir model (Figure 4.25) did not work as well for the post-filter water sample as for DI and the raw water sample. The assumptions for the Langmuir model included monolayer adsorption and homogeneous surface. The latter seem likely for the zeolites being studied as they were manufactured which would allow for a better control over their structural framework, including surface area and pore sizes. There may be monolayer adsorption as well, but the presence of precipitates of compounds like calcium, magnesium and sulfate could be competing with E2 for the adsorption surface area on the zeolites. As a result much lesser mass of E2 would be removed from natural water than from DI where these competing substances are absent.

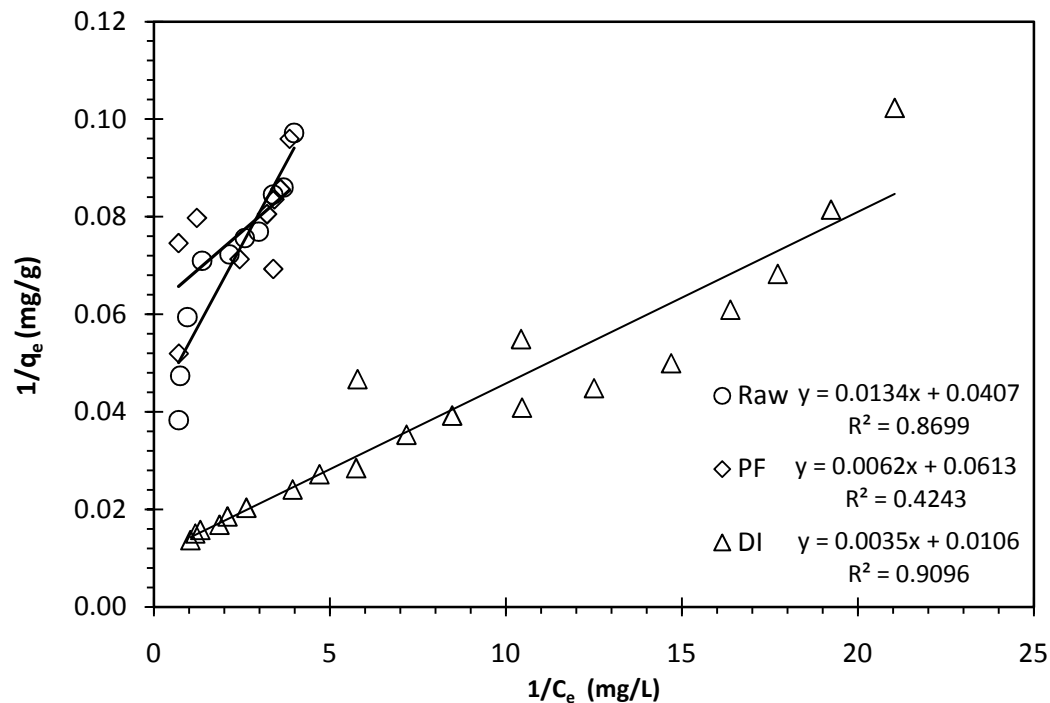


Figure 4.25 The linearized Langmuir isotherm of adsorption of E2 in natural water on CBV-780

The Freundlich and Langmuir parameters obtained for the adsorption of E2 on CBV-780 in natural waters are shown in Table 4.6. The q_{max} value for adsorption in DI water was >3 times the q_{max} values for adsorption in raw water and post filter water, suggesting 3 times as much, or more, zeolites would be needed to remove the same amount of estrogens from the natural water as from DI water.

Table 4.6 Freundlich and Langmuir parameters for deionized and natural waters

Water	Langmuir Parameters		Freundlich Parameters	
	q_{max} (mg/g)	b (L/mg)	$1/n$	K_F [(mg/g)•(L/μg) ^{1/n}]
Deionized	94	3.03	0.588	1.44
Post-filter	16	9.89	0.157	5.0
Raw	25	3.04	0.399	1.2

Attempts were made to regenerate the adsorption capacity of zeolites in natural waters but due to some constraints, experiments could not be completed as successfully as in the case of DI water. The main problem hindering the progress of regeneration cycle was retrieval of zeolites from aqueous solution, which was a necessary step prior to, and after the UV irradiation event. When 40 mg/L of CBV-780 was immersed in natural waters containing E2, as in the case of DI water, it could not be collected through centrifugation. Zeolites formed a very thin sheet along the walls of centrifuge bottles which made the loss of their mass during transfer events unavoidable and much more prominent.

To remedy this factor, more zeolite mass, 100 mg/L was used with the idea of forming thicker layer of zeolites along walls of centrifuge bottles. Doing this made the recovery possible but still a lot of mass was lost such that the experiment could

not be continued beyond 2nd regeneration cycle. However, some data was collected for those experiments but the remaining E2 concentration in the aqueous solution after each adsorption equilibrium increased rather than decreased after every UV irradiation event, suggesting desorption of E2 collected on zeolites from the preceding cycles.

5. SUMMARY AND CONCLUSIONS

Among the zeolites tested for the adsorption capacity for the estrogens- E1, E2 and EE2, CBV-400 showed poor adsorption capacity and hence was screened out from further investigations. CBV-780 and -901 showed much higher adsorption capacities for the target estrogens. The difference in the adsorption capacities of these zeolites was attributed to the Si/Al mole ratio in their molecular structures; the higher the Si/Al mole ratio, the greater was the adsorption capacity. Although CBV-780 and CBV-901 had similar Si/Al ratio, they showed some difference in the adsorption capacity which was explained by the difference in their surface area and the potential variation in their pore structures.

The kinetics of adsorption showed both CBV-780 and -901 achieving >90% reduction in all three estrogen (E1, E2 and EE2) concentrations within the first 10 minutes of the reaction. In general, both the Freundlich and Langmuir isotherm models showed good fit for the data with high correlation coefficients. The Freundlich constant, K_F , and the Langmuir parameter, q_{max} , both indicative of adsorption capacity, did not correlate with Log K_{ow} value which provided a comparison of the hydrophobicity of the adsorbates.

Using UV photolysis and UV/H₂O₂ AOP, the adsorption capacity of CBV-780 was regenerated successfully for 4 regeneration cycles. After 4 regeneration cycles, the UV and UV/H₂O₂ AOP regenerated zeolites cumulatively adsorbed twice or more estrogen (E1, E2 and EE2) mass than the untreated zeolites. The UV and UV/H₂O₂ AOP treatment did not show significant difference in regenerative ability of the zeolites. The difference in the adsorption capacity regenerated with UV and UV/H₂O₂

AOP was <10%. This was explained by the transport issues associated with the hydroxyl radicals formed during UV irradiation and, correspondingly the lack of interaction between the hydroxyl radicals and estrogens adsorbed onto zeolites.

Speculations were also made that excessive UV dose could have been provided, which could efficiently degrade the compounds even in the absence of H₂O₂, given the initial concentration of the contaminant used. Thus, UV irradiance time was reduced from 30 to 5 minutes to investigate if there could be a larger difference in regeneration ability between the UV photolysis and UV/H₂O₂ AOP treatment at lower doses of UV. The results of these experiments also did not show significant difference between the two treatments. This further confirmed the high reactivity and immediate consumption of hydroxyl radical following its formation as the main issue hindering the enhancement of regeneration in the UV/H₂O₂ treatment.

After successful quantification of the adsorption capacities and the regenerative ability of zeolites in deionized water, investigation was done to quantify similar parameters and test the efficacy of the regeneration methodology in natural waters. From a drinking water treatment plant, two sets of water samples were collected: raw water entering the treatment train, and post-filter water which had already undergone coagulation, flocculation and filtration. In natural waters, less E2 was adsorbed by the same amount of zeolites than in DI water. The reduction in the concentration of inorganic carbon, calcium, magnesium and sulfate after the adsorption equilibrium suggested deposition of precipitates of these substances onto zeolites interfering with E2 adsorption.

The consistency of organic matter prior to and after the adsorption equilibrium in both the raw water and post-filter water samples suggested minimal effect of organic carbon on E2 adsorption on zeolites. The amount of dissolved organic carbon in raw water was twice of the amount in post-filter water.

Although, zeolites were able to remove the target estrogens from natural water, the isotherm parameters obtained suggested that a larger zeolite mass (> 3 times) would be required to achieve the same amount of reduction in natural water as in DI water.

6. FUTURE INVESTIGATIONS

In light of the results obtained in this study, some of the future investigations could include:

1. Further examination of the regenerative ability of zeolites in natural water and characterization of dissolved organic matter which could be of similar size and could possibly interact in similar way with the eluent used (1:1 ratio of acetonitrile and DI) in HPLC analysis, exaggerating the perceived aqueous concentration of the estrogens used.
2. Investigation on whether concentrating contaminants in porous media enhances or depresses the effects of UV photolysis.
3. Identification of the byproducts formed during regeneration experiments and assessment of their toxicity.

7. REFERENCES

- Auriol M., Filali-Meknassi Y., Tyagi R.D. (2006). Endocrine disrupting compounds removal from wastewater, a new challenge. *Process Biochemistry* 41: 525-539.
- Beland P. Annual report 1989. Quebec:St. Lawrence National Institute of Ecotoxicology, 1989.
- Bhatia, Subhash. Zeolite Catalysis: Principles and Applications, *CRC Press, Inc.*, Boca Raton, Florida, 1990
- Bishop CA, Brooks RJ, Carey JH, Ng P, Norstrom RJ, Lean DRSJ (1991). The case for a cause-effect linkage between environmental contamination and development in eggs of the common snapping turtle (*Chelydra s. serpentina*) from Ontario, Canada. *J Toxicol Environ Health* 33: 521-548.
- Bolton JR, Linden KG (2003). Standardization of methods for fluence (UV Dose) determination in bench-scale UV experiments. *Journal of Environmental Engineering* © ASCE 3, 209 – 215.
- Chen PJ, Linden KG, Hinton DE, Kashiwada S, Rosenfeldt EJ, Kullman SW (2006). Biological assessment of bisphenol A degradation in water following direct photolysis and UV advanced oxidation. *Chemosphere* 65: 1094-1102.
- Colborn T, Vom Saal FS, Soto AM (1993). Developmental effects of endocrinedisrupting chemicals in wildlife and humans. *Environ Health Perspect* 101:378–84.
- Commission of the European Communities (2001). The implementation of the Community strategy for endocrine disrupters: A range of substances suspected of interfering with the hormone systems of humans and wildlife. *COM [1999]* 706: 45.
- Coughlin RW and F Ezra (1968). Role of surface acidity in the adsorption of organic pollutants on the surface of carbon. *Environmental Science and Technology* 2(4): 291 – 297.
- Davis WP, Bortone SA (1992). Effects of kraft mill effluent on the sexuality of fishes: an environmental early warning? In: Chemically induced alterations in sexual and functional development: the wildlife/human connection (Colbom T, Clement C, eds). Princeton, NJ: *Princeton Scientific Publishing*: 113-127.

- Delle Site, A (2001). Factors affecting sorption of organic compounds in natural sorbent/water systems and sorption coefficients for selected pollutants. A Review. *J. Phys. Chem. Ref. Data* 30 (1): 187 – 439.
- Ellis DV, Pattisina, LA. Widespread neogastropod imposex: a biological indicator of global TBT contamination (1990). *Mar Pollut Bull* 21: 248 – 253.
- Erdman TC. Report to U.S. Fish and Wildlife Service on common and Forster's tern productivity on Kidney Island confined disposal facility, Green Bay, 1987 with supplemental necropsy and pathology reports. Green Bay: University of Wisconsin, 1988.
- Erdem-Şenatalar A, Bergendahl JA, Giaya A, Thompson RW (2004). Adsorption of Methyl Tertiary Butyl Ether on Hydrophobic Molecular Sieves. *Environmental Engineering Science* 21(6): 722 – 729.
- Fry DM, Toone CK DDT-induced feminization of gull embryos. *Science* 231: 919-924(1981).
- Fujita H, Izumi J, Sagehashi M, Fujii T, Sakoda A (2004). Decomposition of trichloroethene on ozone-adsorbed high silica zeolites. *Water Research* 38: 166 – 172.
- Giaya A, Thompson RW, Denkewicz R Jr., (2000). Liquid and vapor phase adsorption of chlorinated volatile organic compounds on hydrophobic molecular sieves. *Microporous and Mesoporous Materials* 40: 205-218.
- Gibbs PE, Pascoe PL, Burt GR (1988). Sex change in the female dog-whelk, *Nucella lapillus*, induced by tributyltin from antifouling paints. *J Mar Biol Assoc UK* 68:715-731.
- Hanselman, T.A., D.A. Graetz, and A.C. Wilkie (2003). Manure-borne estrogens as potential environmental contaminants: A review. *Environ. Sci. Technol.* 37:5471-5478.
- Health Canada (1999). Human health and exposure to chemicals which disrupt estrogen, androgen and thyroid hormone physiology. *Environmental and Occupational Toxicology Division, Environmental Health Directorate, HPB. Tunney's Pasture, P.L., Canada*
- Hu JY, Aizawa T, Ookubo S (2002a). Products of aqueous chlorination of bisphenol A and their estrogenic activity. *Environ Sci Technol* 36(9), 1980–7.
- Hu JY, Xie GH, Aizawa T (Chem 2002b). Products of aqueous chlorination of 4-nonylphenol and their estrogenic activity. *Environ Toxicol* 21(10): 2034–9.

IUVA/IOA –International Ultraviolet Association/International Ozone Association
Regional Conference (May 2009), Cambridge, MA

- Johnson-Restrepo B, Addink R, Wong C, Arcaro K, Kannan K (2007). Polybrominated diphenyl ethers and organochlorine pesticides in human breast milk from Massachusetts, USA. *Journal of Environmental Monitoring* 9) 1205 – 1212.
- Khalid M, Joly G, Renaud A, Magnoux P (2004). Removal of phenol from water by adsorption using zeolites. *Ind. Eng. Chem. Res.* 43: 5275 – 5280.
- Kipling JJ and PV Shooter (1966). The adsorption of iodine vapor by Graphon and Spheron 6. *Journal of Colloid and Interface Science* 21 (2): 238 - 244
- Koryabkina N, Bergendahl JA, Thompson RW, Giaya A (2007). Adsorption of disinfection byproducts on hydrophobic zeolites with regeneration by advanced oxidation. *Microporous and Mesoporous Materials* 104: 77 – 82.
- Kubiak TJ, Harris HJ, Smith LM, Schwartz TP, Stalling DL, Trick JA, Sileo L, Docherty DE, Erdman TC (1989). Microcontaminants and reproductive impairment of the Forster's tern on Green Bay, Lake Michigan-1983. *Arch Environ Contam Toxicol* 18:706-727.
- Lai, K. M., Johnson, K. L., Scrimshaw, M. D. and Lester, J. N. (2000). Binding of waterborne steroid estrogens to solid phases in river and estuarine systems. *Environmental Science and Technology* 34, 3890.
- Leatherland J. Endocrine and reproductive function in Great Lakes salmon. In: Chemically induced alterations in sexual and functional development: the wildlife/human connection (Colborn T, Clement C, eds) (1992). Princeton, NJ: Princeton Scientific Publishing, 129-145.
- Lenz K, Beck V, Fuerhacker M (2004). Behavior of bisphenol A (BPA), 4-nonylphenol (4-NP), and 4-nonylphenol ethoxylates (4-NP1EO, 4-NP2EO) in oxidative water treatment processes. *Water Sci Technol* 50(5), 141–7.
- Linden KG, Rosenfeldt EJ, Johnson S, Melcher B. *Proceedings, AWWA Water Quality Technology Conference*, 2002, Seattle, WA, November 10-14.
- Liu B, Liu X (2004). Direct photolysis of estrogens in aqueous solutions. *Science of the Total Environment* 320, 269.
- Liu JB, Qian CF (1995). Hydrophobic coefficients of s-triazine and phenylurea herbicides. *Chemosphere* 31(8): 3951–3959.

- LOGKOW©- A databank of evaluated octanol-water partition coefficients (Log P), (accessed in April 2010).
< <http://logkow.cisti.nrc.ca/logkow/display?OID=19500>>
- López de Alda MJ, Barceló D (2001). Review of analytical methods for the determination of estrogens and progestogens in waste waters. *Fresenius J Anal Chem* (371): 437 – 447.
- Mac MJ, Schwartz T, Edsall CC. Correlating PCB effects on fish reproduction using dioxin equivalents. Presented at the Ninth Annual Society of Environmental Toxicology and Chemistry Meeting, Arlington, Virginia, 1988.
- Marcilly, Ch (2001). Evolution of Refining and Petrochemicals. What is the place of zeolites. *Stud. Surf. Sci. Catal.*, 135: 37.
- Martineua D, Lagace A, Beland P, Higgins R, Armstrong D, Shugart LR (1988). Pathology of stranded beluga whales (*Delphinapterus kucas*) from the St. Lawrence estuary, Quebec, *Canada. J Comp Pathol* 98:287-311.
- Moccia R, Fox G, Britton AJ (1986). A quantitative assessment of thyroid histopathology of herring gulls (*Larus argentatus*) from the Great Lakes and a hypothesis on the causal role of environmental contaminants. *J Wild Dis* 22:60-70.
- Moccia RD, Leatherland JF, Sonstegard RA. Quantitative interlake comparison of thyroid pathology in Great Lakes coho (*Oncorhynchus kisutch*) and chinook (*Oncorhynchus tshawytscha*) salmon. *Cancer Res* 41:2200-2210 (1981).
- Munkittrick KR, Port CB, Van Der Kraak GJ, Smith IR, Rokosh DA. Impact of bleached kraft mill effluent on population characteristics, liver MFO activity, and serum steroids of a Lake Superior white sucker (*Catostomus commersoni*) population. *Can J Fish Aquat Sci* 48:1-10(1991).
- Ohko Y, Iuchi K-I, Niwa C, Tatsuma T, Nakashima T, Iguchi T (2002). 17 β -estradiol degradation by TiO₂ photocatalysis as a means of reducing estrogenic activity. *Environmental Science and Technology* 36, 4175.
- Okkerman PC and CP Groshart (2001). Chemical study on estrogens. BKH Consulting Engineers, RIKZ, Netherlands
- Petrovic, M., Eljarrat, E., López De Alda, M.J., Barceló, D., (2004). Endocrine disrupting compounds and other emerging contaminants in the environment: a survey on new monitoring strategies and occurrence data. *Anal. Bioanal. Chem.* 378, 549–562.

- Poerschmann J, Gorecki T, Kopinke FD (2000). Sorption of very hydrophobic organic compounds onto poly(dimethylsiloxane) and dissolved humic organic matter. 1. Adsorption or partitioning of VHOC on PDMS-coated solid-phase microextraction fibers—a never-ending story? *Environ Sci Technol* 34(17): 3824–30.
- Rao BH, Asolekar SR (2001). QSAR models to predict effect of ionic strength on sorption of chlorinated benzenes and phenols at sediment–water interface. *Water Res*; 35(14): 3391–401.
- Reijnders PJH. Reproductive failure in common seals feeding on fish from polluted coastal waters (1986). *Nature* 324:456-457.
- Reungoat J, Pic JS, Manéro MH, Debellefontaine H (2007). Adsorption of nitrobenzene from water onto high silica zeolites and regeneration by ozone. *Separation Science and Technology*, 42: 1447 – 1463.
- Rosenfeldt EJ, Chen PJ, Kullman S, Linden KG (2007). Destruction of estrogenic activity in water using UV advanced oxidation. *Science of the Total Environment* 377; 105-113.
- Rosenfeldt EJ, Linden KG, Canonica S, Gunten UV (2006). Comparison of the efficiency of $\cdot\text{OH}$ radical formation during ozonation and advanced oxidation processes $\text{O}_3/\text{H}_2\text{O}_2$ and $\text{UV}/\text{H}_2\text{O}_2$. *Water Research* 40; 3695-3705.
- Rosenfeldt EJ, Milcher B, Linden KG. UV and $\text{UV}/\text{H}_2\text{O}_2$ treatment of methylisoborneol (MIB) and geosmin in water (2005). *J Water Supply Res Technol-AQUA* 54 (7): 423-34.
- Rosenfeldt EJ and Linden KG (2004). Degradation of endocrine disrupting chemicals bisphenol A, ethinyl estradiol, and estradiol during UV photolysis and advanced oxidation processes. *Environmental Science and Technology* 38(20): 5476-5483
- Sagehashi M, Shiraishi K, Fujita H, Fujii, Sakoda A (2005). Ozone decomposition of 2-methylisoborneol (MIB) in adsorption phase on high silica zeolites with preventing bromated formation. *Water Research*, 39 (13): 2926 – 2934.
- SET- Spartan Environmental Technologies (accessed February 2010). Ozone Generators and Advanced Oxidation Processes, available at < <http://www.spartanwatertreatment.com/index.html>>
- Sharpless CM, Linden KG (2001). UV photolysis of nitrate: effects of natural organic matter and dissolved inorganic carbon and implications for UV water disinfection. *Environ Sci Technol* 35; 2949-55.

- Sharpless CM, Linden KG (2003). Experimental and model comparisons of low- and medium-pressure Hg lamps for the direct and H₂O₂ assisted UV photodegradation of *N*-Nitrosodimethylamine in simulated drinking water. *Environ Sci Technol* 37 (9): 1933-40.
- Shugart G (1978). Frequency and distribution of polygony in Great Lakes herring gulls *Condor* 82:426-429(1980).
- Sharpless CM, Linden KG, (2001). "UV Photolysis of Nitrate: Effects of Natural Organic Matter and Dissolved Inorganic Carbon and Implications for UV Water Disinfection" *Environmental Science and Technology* 35 (14), 2949
- Singer P, Reckhow D (1999). Chemical oxidation In: Water Quality and Treatment: A Handbook of Community Water Supplies. *McGraw-Hill, Inc.* New York, USA.
- Snoeyink VL and RS Summers (1999). Water Quality and Treatment: A Handbook of Community Water Supplies, Chapter 13- Adsorption of Organic Compounds. *McGraw-Hill Companies*, New York, USA.
- Snyder SA, Keith TL, Verbrugge DA, Snyder EM, Gross TS, Kannan K, and Giesy JP (1999). Analytical methods for detection of selected estrogenic compounds in aqueous mixtures. *Environmental Science and Technology* 33: 2814.
- Snyder SA, Villeneuve DL, Snyder EM, and Giesy JP (2001). Identification and quantification of estrogen receptor agonists in wastewater effluents. *Environmental Science and Technology* 35: 3620.
- Snyder, S.A., Westerhoff, P., Yoon, Y., and Sedlak, D.L. (2003). Pharmaceuticals, personal care products, and endocrine disruptors in water: implications for the water industry. *Environmental Engineering Science* 20, 449-469
- Takasugi N, Bern HA (1988). Introduction: abnormal genital tract development in mammals following early exposure to sex hormones. In: Toxicity of hormones in perinatal life (Mori T, Nagasawa H, eds). *Boca Raton, FL: CRC Press*, 1-7.
- Tanaka H, Yakou Y, Takahashi A, Higashitani T and Komori K (2001). Comparison between estrogenicities estimated from DNA recombinant yeast assay and from chemical analyses of endocrine disruptors during sewage treatment. *Water Science and Technology* 43: 125.
- Tsai WT, Hsu HC, Su TY, Lin KY, Lin CM (2006). Adsorption characteristics of bisphenol-A in aqueous solutions onto hydrophobic zeolite. *Journal of Colloid and Interface Science* 299: 513 – 519.

- USEPA 1999. EPA Guidance Manual
http://www.epa.gov/ogwdw000/mdbp/pdf/alter/chapt_8.pdf
- Van den Belt K., Berckmans P., Vangenechten C., Verheyen R., Witters H. (2004). Comparative study on the in vitro/in vivo estrogenic potencies of 17 β -estradiol, estrone, 17 α -ethynylestradiol and nonylphenol. *Aquatic Toxicology* 66, 183-195.
- Wells MJM, Pellegrin ML, Morse A, Bell KY, Fono LJ (2008). Emerging Pollutants. *Water Environment Research* 80 (10): 2026 – 2057.
- Wen H, Bergendahl JA, Thompson RW (2009). Removal of estrone from water by adsorption on zeolites with regeneration by direct UV photolysis. *Environmental Engineering Science* 26(2): 319 – 326.
- Westerhoff P, Yeomin Y, Shane S, Wert E (2005). Fate of Endocrine-Disruptor, Pharmaceutical, and Personal Care Product Chemicals during Simulated Drinking Water Treatment Process. *Environmental Science Technology* 39, 6649-6663.
- Yoon, Y., Westerhoff, P., Snyder, S. A. and Wert, E. C. (2006). Nanofiltration and ultrafiltration of endocrine disrupting compounds, pharmaceuticals and personal care products. *Journal of Membrane Science* 270, 88.

Appendix A – Suppliers Information on the Zeolites Tested

ZEOLYST INTERNATIONAL

Certificate of Analysis

Account

Order number

Product CBV400

Lisnumber 400054002618

Ao (Å) 24.52

wt% Na₂O (ignited) 2.37

Ratio (SiO₂/Al₂O₃) 5.21

wt% SiO₂ (ignited) 73.24

wt% Al₂O₃ (ignited) 23.86

LOI (1 hour, 1000° C) 5.4

SA (BET at p/po = 0,03) 817

Oosterhorn 36, 9936 HD Delfzijl, The Netherlands

Tel: +31 (0)596-643311 Fax: +31 (0)596-630392

Beate.Tkacz@zeolyst.nl

www.zeolyst.com

23-4-2009

Page 1 of 1

Certificate of Analysis

Account

Order number

Product	CBV780
---------	--------

Lisnumber	78004N000508
-----------	--------------

Ao (Å)	24.24
--------	-------

wt% Na ₂ O (ignited)	0.01
---------------------------------	------

Ratio (SiO ₂ /Al ₂ O ₃)	80.92
---	-------

wt% SiO ₂ (ignited)	97.93
--------------------------------	-------

wt% Al ₂ O ₃ (ignited)	2.054
--	-------

LOI (1 hour, 1000° C)	9.6
-----------------------	-----

SA (BET at p/po = 0,03)	861
-------------------------	-----

Oosterhorn 36, 9936 HD Delfzijl, The Netherlands

Beate.Tkacz@zeolyst.nl

Tel: +31 (0)596-643311 Fax: +31 (0)596-630392

www.zeolyst.com

10-9-2009

Page 1 of 1

ZEOLYST

INTERNATIONAL

Product Analysis Sheet

<i>Product Code</i>	CBV 901
<i>Zeolite Type</i>	Y Zeolite
<i>Lot #</i>	2200-56
<i>XRF</i>	
<i>%Na₂O (wt.%)</i>	0.01
<i>SiO₂/Al₂O₃ (molar ratio)</i>	82.6
<i>XRD</i>	
<i>Unit Cell Size Å</i>	24.2
<i>% Crystallinity</i>	119
<i>Surface Area</i>	
<i>Multi Point (m²/g)</i>	743
<i>Particle Size</i>	
<i>D₅₀ microns</i>	4.3
<i>D₉₀ microns</i>	17
<i>Adsorption</i>	
<i>Hydrophobicity Index</i>	30

APPENDIX B – Medium Pressure Lamp



Medium Pressure quasi-collimated beam batch reactor setup

APPENDIX C – MP UV Photolysis of EDCs selected

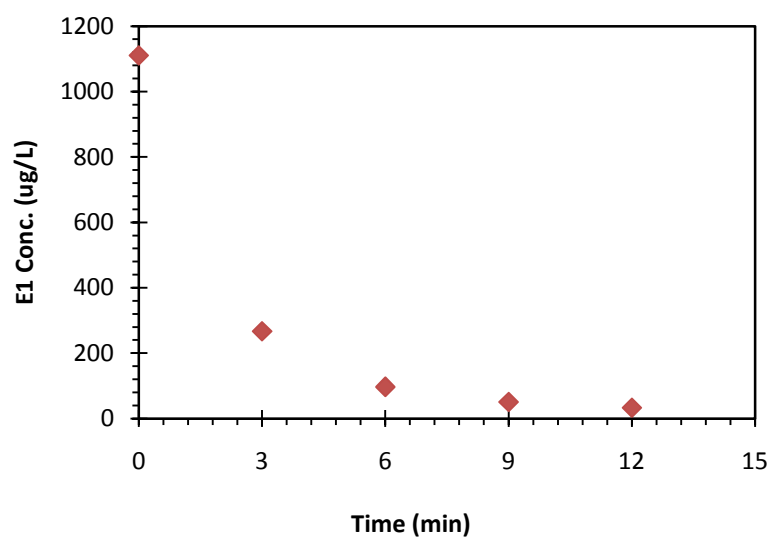


Figure C-1. Degradation of estrone (E1) when irradiated with MP UV source.

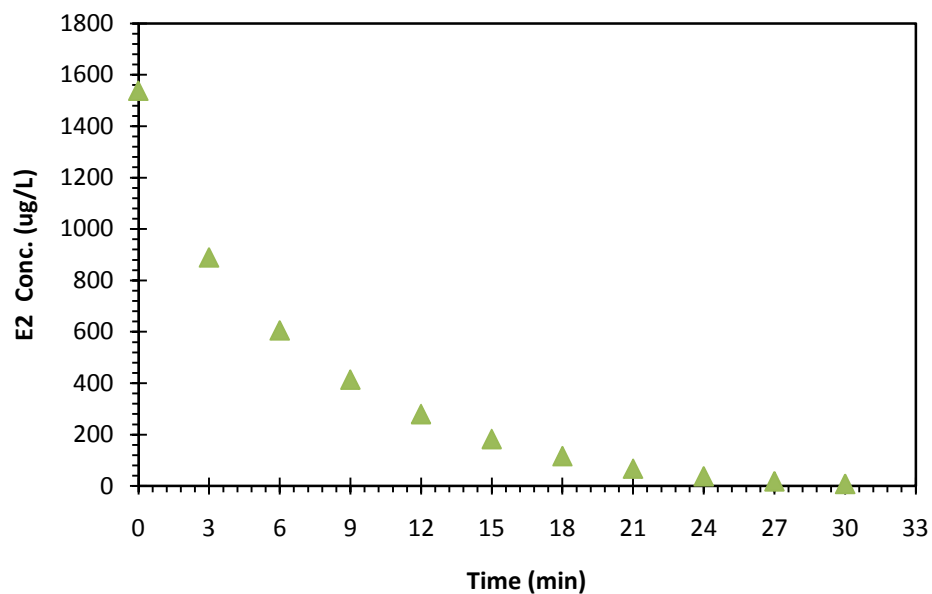


Figure C-2 Degradation of 17-β-estradiol (E2) when irradiated with MP UP source

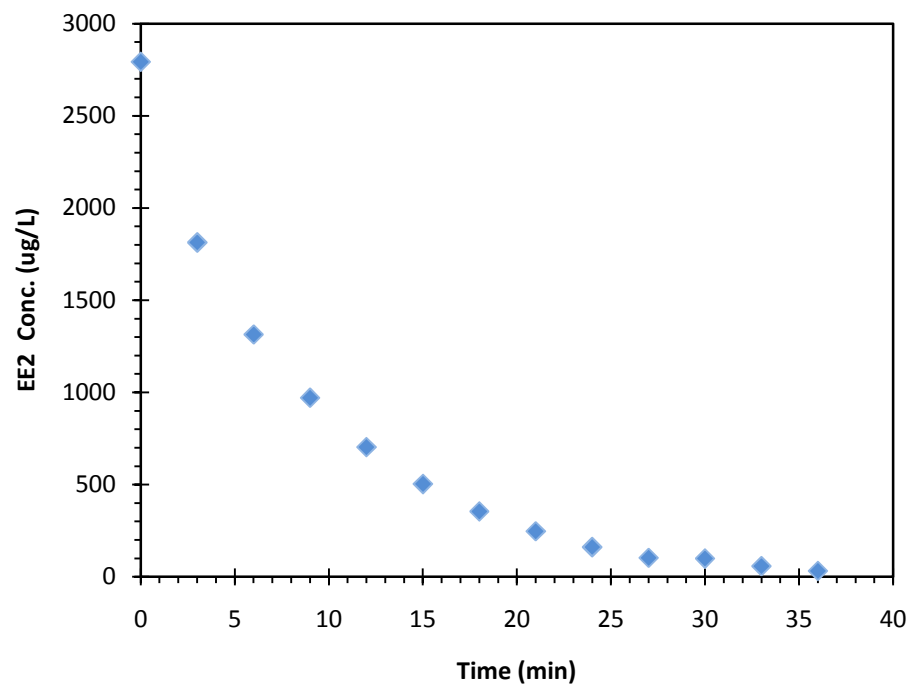


Figure C-3. Degradation of 17- α -ethinylestradiol when irradiated with MP UV source

APPENDIX D – E1, E2 and EE2 Calibration Curves

E1 - 5 to 10000 ug/L

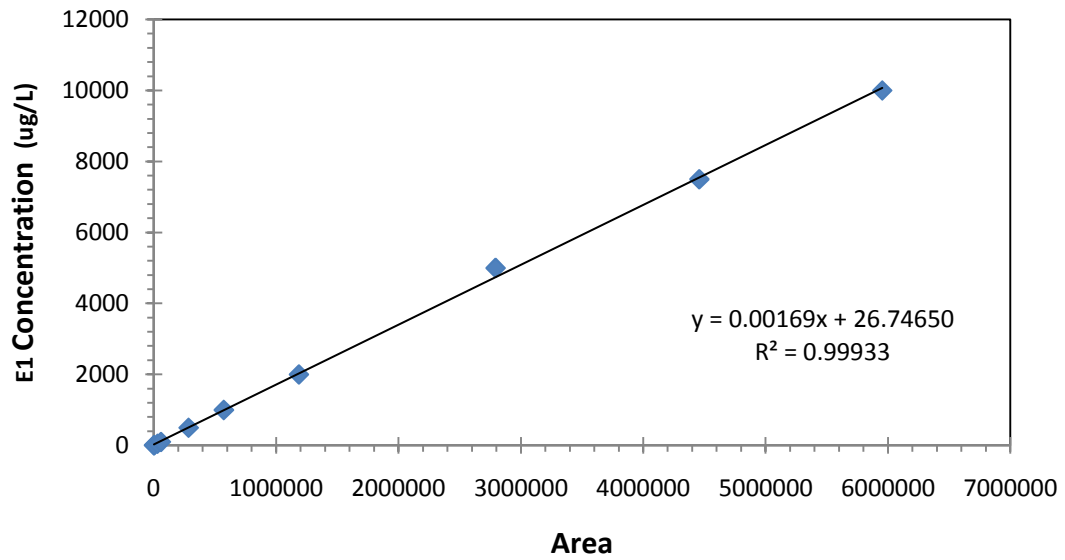


Figure B-1 Calibration curve for estrone (E1)

E2 - 5 to 2000 ug/L

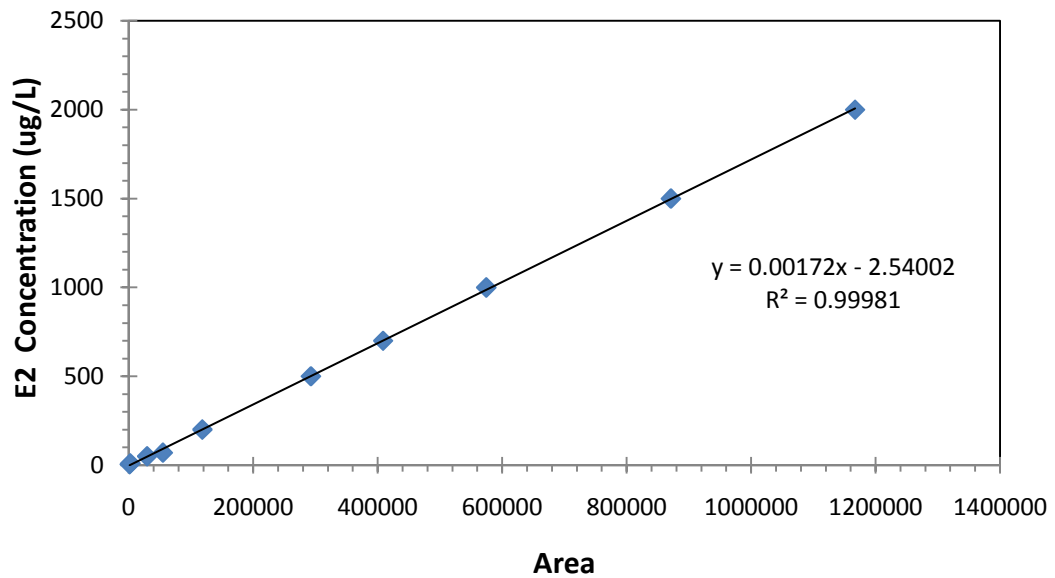


Figure B-2. Calibration Curve for 17β-estradiol (E2)

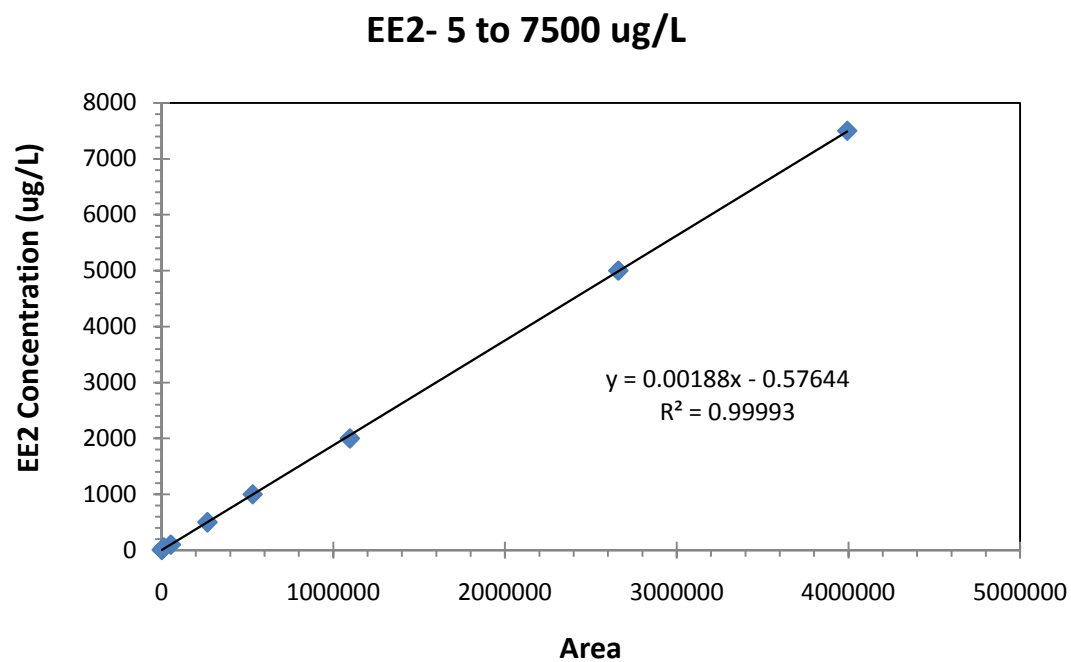


Figure B-3. Calibration curve for 17- α - ethinylestradiol (EE2)

APPENDIX E – Detection Limit of Water Quality Analysis Equipments Used

Equipments	Contents	Detection Limit	Max Limit
ICP	Sodium	0.06 mg/L	100 mg/L
	Potassium	0.04 mg/L	20 mg/L
	Magnesium	0.01 mg/L	75 mg/L
	Calcium	0.01 mg/L	75 mg/L
	Iron	0.01 mg/L	50 mg/L
IC	Chloride	0.03 mg/L	1000 mg/L
	Sulfate	0.09 mg/L	250 mg/L
	Nitrate	0.05 mg/L	25 mg/L
	Phosphate	0.10 mg/L	25 mg/L
TOC (Shimadzu)	Inorganic Carbon	0.60 mg/L	100 mg/L
	Organic Carbon	0.1- 0.3 mg/L	10 mg/L